0 mV and the conductance is selective to cations in GDPβs-loaded cells. P2X agonists produced a rapidly desensitizing response in NHEK as well as in DRG neurons (Grubb and Evans, 1999). Furthermore, the ATP-evoked increase of $[Ca^{2+}]_i$ was influenced by the absence of extracellular Ca^{2+} in differentiating over-confluent cells.

P2X receptors were classified within several subtypes, based on their sensitivity to agonists and antagonists, or the time course of their desensitization because of currents (Evans and Surprenant, 1996). $P2X_1$ and $P2X_3$ receptors are characterized by their sensitivity to αβ-meATP and a rapidly

desensitizing current. $P2X_2$ and $P2X_{4-7}$ receptors are characterized by insensitivity to αβ-meATP and a slowly desensitizing current. Although homomeric $P2X_2$ receptors are insensitive to αβ-meATP, heteromeric $P2X_{2/3}$ receptors are characterized by their sensitivity to αβ-meATP and a slowly desensitizing current (Lewis *et al*, 1995; Ueno *et al*, 1998). Additionally, the responses of the currents are categorized by their sensitivity to the P2X antagonist PPADS. PPADS antagonized $P2X_1$, $P2X_2$, $P2X_3$, $P2X_{2/3}$, $P2X_5$, and $P2X_7$, but not $P2X_4$ or $P2X_6$. In this study, αβ-meATP-activated currents have the following features: their responses may be rapidly or slowly desensitizing currents; the slowly desensitizing currents were inhibited by PPADS and TNP-ATP. These results suggest that $P2X_1$, $P2X_{2/3}$, and $P2X_3$ receptors were responsible for the responses. ATP-activated currents that yield slowly desensitizing responses have the following features: these responses were insensitive to αβ-meATP, and inhibited by PPADS. ATP-activated current with a slowly desensitizing response however was not inhibited by PPADS in some of cells. Furthermore, the current responses attained because of BzATP and 2MeSATP support our characterization of $P2X_2$, $P2X_4$, $P2X_5$, and/or $P2X_7$. Although it is evident from the results of current responses and RT-PCR that $P2X_1$, $P2X_{2/3}$, $P2X_3$, $P2X_4$, and $P2X_5$ receptors are functional in proliferating subconfluent cells, their contribution seems minimal as the ATP-evoked increases of $[Ca^{2+}]_i$ were not influenced by the absence of extracellular Ca^{2+} in proliferating subconfluent cells (Fig 3). Furthermore, UTP and ATP evoked the same increases of $[Ca^{2+}]_i$ in the presence of extracellular Ca^{2+}. These results coincide with previous researches that indicated that it is the $P2Y_2$ receptors that play a functional role in the proliferated phase (Dixon *et al*, 1999; Lee *et al*, 2001; Burrell *et al*, 2003; Greig *et al*, 2003). Although UTP activates $P2Y_2$ and $P2Y_4$ receptors, the $P2Y_4$ subtype is a functional receptor in HaCaT keratinocytes but not in NHEK (Burrell *et al*, 2003).

$P2Y_2$ receptors respond to ATP in the proliferated phase; however, in the differentiated phase, it is the P2X receptors that mediate a greater response from ATP (Fig 3). Only differentiated over confluent cells were affected by the absence of extracellular Ca^{2+}. There were higher increases
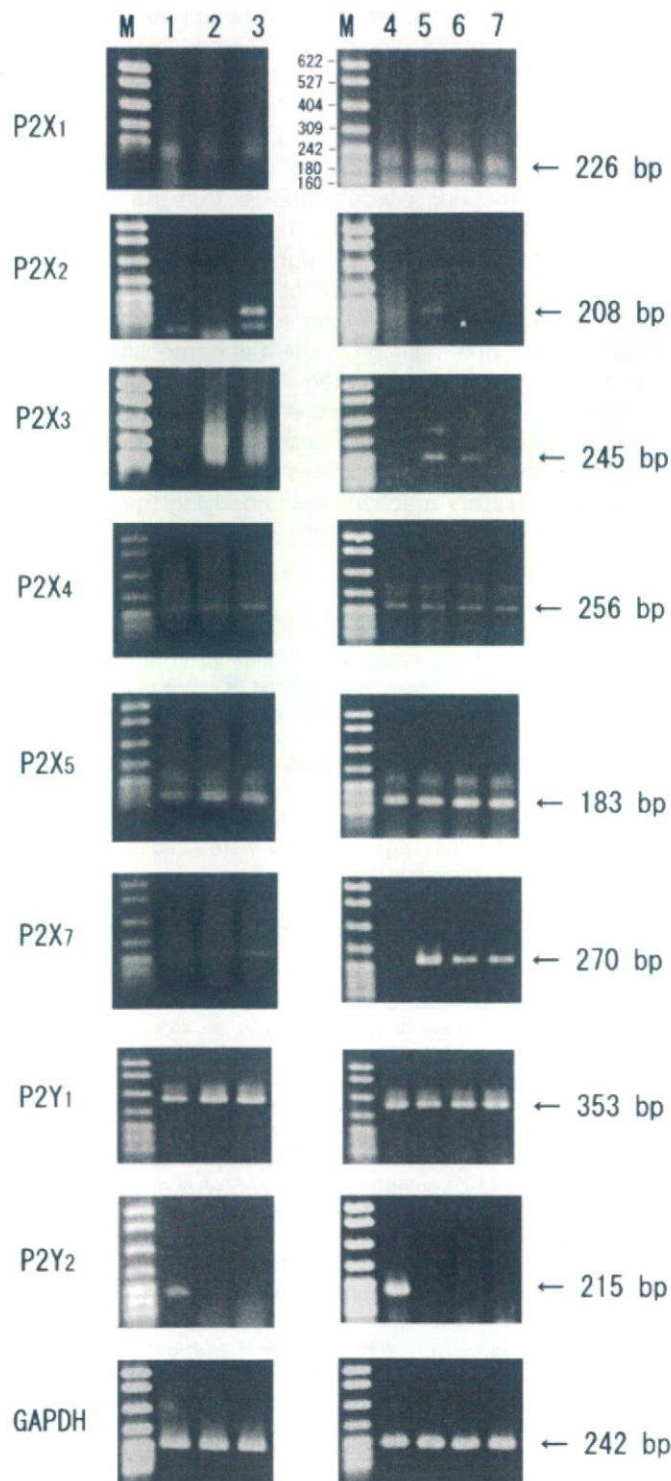

Figure 4
Changes in P2X and P2Y receptor subtype mRNA expressions in different conditions of normal human epidermal keratinocytes (NHEK). The left panels indicate that P2 receptor mRNA expression is affected by each culture condition. The right panels indicate that P2 receptor mRNA expression is affected while exposed to ATP and UVB radiation. Arrows indicate the PCR amplification products corresponding to P2X and P2Y receptor subtypes. M, DNA size markers; lane 1, proliferating subconfluent keratinocytes; lane 2, differentiating over-confluent keratinocytes; lane 3, differentiating over-confluent keratinocytes on addition of Ca (1.8 mM); lane 4, proliferating subconfluent keratinocytes; lane 5, proliferating subconfluent keratinocytes exposed to ATP (300 μM) for 6 h; lane 6, proliferating subconfluent keratinocytes exposed to UVB (60 mJ per cm²); lane 7, proliferating subconfluent keratinocytes exposed to UVB (30 mJ per cm²). Cytotoxicity was not found in any of the cell conditions (proliferating subconfluent keratinocytes; lanes 1 and 4, 1017 ± 52, n = 6, differentiating over-confluent keratinocytes; lane 2, 1152 ± 29, n = 6, differentiating over-confluent keratinocytes on addition of Ca; lane 3, 1173 ± 47, n = 6, proliferating subconfluent keratinocytes exposed to ATP for 6 h; lane 5, 1027 ± 43, n = 6, proliferating subconfluent keratinocytes exposed to UVB (60 mJ per cm²); lane 6, 1025 ± 64, n = 6, proliferating subconfluent keratinocytes exposed to UVB (30 mJ per cm²); lane 7, 1003 ± 41, n = 6).

of response to $\alpha\beta$-meATP and BzATP in differentiating over-confluent cells. On the other hand, the responses to ATP, UTP, and 2MeSADP decreased in the differentiated phase. Although the 2MeSADP-evoked $[Ca^{2+}]_i$ decreased in confluent cells, P2Y$_1$ expression remained unchanged. At this point however, we cannot distinguish the inconsistency between the expression level and Ca^{2+} response. Although 2MeSADP is also an agonist for P2Y$_{12}$, and P2Y$_{13}$, ADP, an agonist for P2Y$_1$, P2Y$_{12}$, and P2Y$_{13}$, elevated $[Ca^{2+}]_i$ in HaCaT keratinocytes but not in NHEK (Burrell et al, 2003). Thus, it is unlikely that these receptors are functional. Although the expression of P2Y$_2$ mRNA was downregulated at the differentiated phase, the expression of multiple P2X$_2$, P2X$_3$, P2X$_5$, and P2X$_7$ receptor subtype mRNA increased (Fig 4). Judging from the results of Ca^{2+} responses and RT-PCR, P2X$_3$ and P2X$_7$ receptor subtypes mainly function in the differentiated phase. The variation of multiple P2X receptor expression in cultured keratinocytes supports the notion that the P2X$_5$ and P2X$_7$ receptors are localized in the differentiated or terminal differentiated skin (Greig et al, 2003).

P2X$_3$ receptors are known to be selectively expressed in a subpopulation of small diameter sensory neurons (Chen et al, 1995; Lewis et al, 1995). P2X$_3$ receptors however, have been observed in nonneuronal cells, such as thymus (Glass et al, 2000) and urothelial cells (Sun and Chai, 2004). Stretching in bladder urothelial cells increased P2X$_3$ receptor expression and their expression was increased more in urothelial cells from patients with interstitial cystitis than that in control subjects (Sun and Chai, 2004). The epidermis could be an interface of the body and environment; hence, the P2X receptors may play a role as some kind of sensor against multiple environmental factors such as barrier disruption and UV radiation. P2X$_7$ receptors are known to be involved in ATP-induced apoptosis (Ferrari et al, 1997). P2X$_7$ receptors are likely to be part of the machinery of the end-stage terminal differentiation of keratinocytes (Greig et al, 2003). Extracellular ATP increased P2X$_1$, P2X$_2$, P2X$_3$, and P2X$_7$ receptors but not P2X$_4$, P2X$_5$ expression (Fig 4). UVB radiation also induces apoptosis in keratinocytes (Schwarz et al, 1995). In this study, P2X$_1$, P2X$_3$, and P2X$_7$ receptor expression, but not P2X$_2$ receptor expression, was augmented by UVB radiation. P2X$_4$, P2X$_5$, and P2Y$_1$ receptors expression however, was unaffected by ATP or UVB radiation. P2Y$_2$ receptor expression was downregulated by the application of ATP and UVB radiation. The downregulation of P2Y$_2$ receptors expression shows that extracellular ATP and UVB radiation inhibited proliferation. A high concentration of ATP inhibits proliferation and a low concentration of ATP promotes proliferation (Dixon et al, 1999; Greig et al, 2003).

We demonstrated that P2X receptors were nonselective cationic channels; on the other hand, the response to ATP mediated through P2Y receptors activated Cl$^-$ conductance. Ca^{2+}-activated Cl channel and K channel contributed to the hyperpolarization induced by ATP, bradykinin, and histamine in HaCaT keratinocytes (Koegel and Alzheimer, 2001). Mauro et al, (1990) described that Cl$^-$ conductance, increased by elevating extracellular Ca^{2+}, plays a role in the initiation of differentiation. Increases in $[Ca^{2+}]_i$ and phosphatidylinositol turnover because of the elevation of extra-

cellular Ca^{2+} were important components of the signal for differentiation (Jaken and Yuspa, 1988; Hennings et al, 1989). These studies suggest the possibility that the intracellular Ca^{2+} released from IP$_3$-sensitive stores affects Cl$^-$ conductance and resultantly leads to keratinocyte differentiation. With these studies as a background, it shall be assumed that Cl$^-$ conductance via P2Y receptors also contributes to the initiation of differentiation. This ionic selectivity of P2 receptor subtypes may be associated with the localization in skin and contribute to the maintenance of homeostasis in skin.

Furthermore, a difference in the amount of released ATP or the localization of P2 receptors between normal healthy subjects and patients would be expected. ATP released from uroepithelial cells was higher in patients with interstitial cystitis than in controls (Sun et al, 2001). Since mechanical scratching has the potential to induce the release of a large amount of ATP release in atopic or psoriatic skin and leads to skin inflammation, it would appear that the purinergic signaling is clinically significant. The stimulation of ATP occurs throughout all stages, through proliferation, differentiation, and apoptosis. Regulation of P2 receptor subtypes is necessary in order to control ion influx and membrane potential, which helps maintain epidermal homeostasis.

In summary, we demonstrated the presence of functional multiple P2X receptors in NHEK, suggesting their important physiological role as an initial sensor for external stimuli. P2 receptor subtypes in keratinocytes would provide a basis to study the regulatory mechanisms underlying the differentiation and proliferation of keratinocytes.

Materials and Methods

Cells and cell culture NHEK (10 Strains of NHEK) were purchased from Kurabo (Osaka, Japan). NHEK were cultured in serum-free keratinocyte growth medium, consisting of Humedia-KB2 (Kurabo) supplemented with bovine pituitary extract (0.4% vol/vol), human recombinant epidermal growth factor (0.1 ng per mL), insulin (10 μg per mL), and hydrocortisol (0.5 μg per mL). The medium was replaced every 2–3 d. For the electrophysiological experiments, NHEK (passage 1–3 cells) were seeded onto collagen-coated glass coverslips and used within 4 d.

Electrophysiological recordings Membrane currents were measured using whole-cell clamp techniques (Hamill et al, 1981). Cells that were grown on collagen coated-cover slips were transferred to an experimental chamber of about 1 mL volume. The chamber was continuously perfused with an extracellular solution containing (in mM) NaCl 140, KCl 5.4, CaCl$_2$ 1.8, MgCl$_2$ 1.0, 10.0 N-2-hydroxyethylpiperazine-N-2-ethanesulfonic acid (HEPES), 11.1 D-glucose (adjusted with NaOH to pH 7.4). Heat-polished patch pipettes had a tip resistance of 3–5 MΩ when filled with an intracellular solution containing 150 mM CsCl, 1 mM MgCl$_2$, 10 mM HEPES, and 5 mM-glycoletherdiamine N,N,N,N-tetraacetic acid (pH 7.2 with CsOH). Intracellular solution was supplemented with 0.3 mM guanosine 5'triphosphate (GTP) or 2 mM guanosine 5'-O-(2-thiodiphosphate) trilitium salt (GDPβS). To exclude the P2Y-activated current, GDPβS, an inhibitor of GTP-binding protein, was applied to the cells (Nakazawa, 1994). Three hundred millimolar KCl-agar bridge electrode was used as the reference electrode. Cell capacitance was compensated after the whole-cell mode was obtained. Cells were clamped at −60 mV. A step pulse between −100 and +40 mV was applied to the cell. Membrane currents were recorded with a patch-clamp amplifier (Axopatch 200B, Axon Instruments, Union City, California). Electrical signals were filtered

at 1 kHz. Current signals were stored in a personal computer and analyzed using pCLAMP 6.0 and Clampfit 6.0 software (Axon Instruments). The drugs were dissolved in the extracellular solution and applied to the cells by perfusion. The experiments were performed at room temperature ($\sim 25^\circ$C). TNP-ATP was purchased from Molecular Probes (Eugene, Oregon). All other chemicals were purchased from Sigma-Aldrich (St Louis, Missouri).

Ca^{2+} imaging in single keratinocyte NHEK were grown to approximately 60%–80% confluency (subconfluent), 100%–120% confluency (confluent), and 100%–120% confluency at 48 h post-treatment with 1.8 mM Ca^{2+} (confluent + Ca) on collagen-coated cover glass chambers (Nalge Nunc, Naperville, Illinois). Changes in $[Ca^{2+}]_i$ in single cell were measured by the fura-2 method as described by Grynkiewicz *et al* (1985) with minor modifications (Koizumi and Inoue, 1997). In brief, the culture medium was replaced with a balanced salt solution (BSS) of the following composition (mM): NaCl 150, KCl 5, CaCl$_2$ 1.8, MgCl$_2$ 1.2, HEPES 25, and D-glucose 10 (pH = 7.4). Cells were loaded with 5 μM fura-2 acetoxymethylester (fura-2AM) (Molecular Probes) at room temperature ($\sim 25^\circ$C) in BSS for 45 min, followed by a BSS wash and a further 15 min incubation to allow de-esterification of the loaded dye. The coverslip was mounted on an inverted epifluorescence microscope (IX70, TS Olympus, Tokyo, Japan), equipped with a 75 W xenon-lamp and band-pass filters of 340 and 380 nm wavelengths. The image data, recorded by a high-sensivity CCD (charge-coupled-device) camera (ORCA-ER, Hamamatsu Photonics, Hamamatsu, Japan) were regulated by a Ca^{2+} analyzing system (AQUACOSMOS/RATIO, Hamamatsu Photonics). In the Ca^{2+}-free experiments, Ca^{2+} was removed from the BSS and 1 mM EGTA was added. Nucleotides were dissolved in the BSS and the cells were exposed to it by method of perfusion. Data were represented as the ratio of fluorescence intensities of 340 and 380 nm.

The preparation for total RNA extraction and synthesis cDNA For RT-PCR studies, NHEK were grown in 10 cm collagen-coated dish (Asahi Techno Glass, Tokyo, Japan) to 60%–80% confluency (subconfluent), 100%–120% confluency (confluent), and 100%–120% confluency at 48 h post-treatment with 1.8 mM Ca^{2+} (confluent + Ca). Sixty to eighty percent confluency cells collected at 6 h post-treatment with UVB (30 and 60 mJ per cm^2) and ATP (300 μM). While using UV radiation, the medium was replaced by PBS (–). NHEK were exposed to UVB radiation from a bank of two Toshiba FL 20 SE sunlamps (Toshiba Electric, Tokyo, Japan). These tubes emit wavelengths between 280 and 340 nm, with a peak of 304 nm. Radiance was measured by a UV-Radiometer (Topcon, Tokyo, Japan). After exposing NHEK to radiation, the medium was added back to the dishes and NHEK were incubated at 37°C in 5% CO_2 for 6 h. ATP was applied with medium for 6 h at 37°C in 5% CO_2. Total RNA was isolated from all individual samples using ISOGEN (Nippon Gene, Osaka, Japan) according to the manufacturer's protocol. We synthesized cDNA from 1 μg of total RNA by the use of 200 U of M-MLV RT (Invitrogen, Carisbad, California) in 20 μL of reaction mixture containing 0.5 μg of oligo (dT) primer (Invitrogen), 50 mM Tris-HCl, pH 8.3, 75 mM KCl, 3 mM MgCl$_2$, 10 mM dithiothreitol, 0.25 mM dATP, 0.25 mM dTTP, 0.25 mM dGTP, 0.25 mM dCTP (Takara, Japan), and 50 U of ribonuclease inhibitor (Takara, Otsu, Japan) at 37°C for 1 h.

RT-PCR The amounts of P2 receptors and human GAPDH cDNA in samples were amplified by using an ABI PRISM 7700 sequence detector (Applied BioSystems, Foster City, California). The reaction mixture was as follows: PCR buffer, 3.5 mM MgCl$_2$, 0.2 μM forward primer, 0.2 μM reverse primer, 0.2 mM dNTP, and 1.25 U of AmpliTaq Gold DNA polymerase (Applied BioSystems). The PCR conditions were: 50°C for 2 min; 95°C for 10 min; 35 cycles of 95°C for 15 s; and 60°C for 1 min. Obtained DNA fragments by PCR

Table I. Primers list of P2 receptors and glyceraldehydes-3-phosphate dehydrogenase (GAPDH)

Gene	Primers (forward and reverse)	Accession number in GenBank	Product size (bp)
P2X$_1$	5′-CCAGCTTGGCTACGTGGTGCAAGA-3′	U45448	226
	5′-ACGGTAGTTGGTCCCGTTCTCCACAA-3′		
P2X$_2$	5′-CCCGAGAGCATAAGGGTCCACAAC-3′	AF190823	208
	5′-AATTTGGGGCCATCGTACCCAGAA-3′		
P2X$_3$	5′-CCCCTCTTCAACTTTGAGAAGGGA-3′	NM002559	245
	5′-GTGAAGGAGTATTTGGGGATGCAC-3′		
P2X$_4$	5′-CCTTCCCAACATCACCACTACTTACC-3′	U85975	256
	5′-AGGAGATACGTTGTGCTCAACGTC-3′		
P2X$_5$	5′-AGCACGTGAATTGCCTCTGCTTAC-3′	AF016709	183
	5′-ATCAGACGTGGAGGTCACTTTGCTC-3′		
P2X$_6$	5′-ATGGCCCTGTCCAAGTTCTGACAC-3′	AF065385	140
	5′-TGTTGCCTCATCCTTGCTTTCGCT-3′		
P2X$_7$	5′-CTGCTCTCTTGAACAGTGCCGAAA-3′	Y09561	270
	5′-AGTGATGGAACCAACGGTCTAGGT-3′		
P2Y$_1$	5′-ACCTCAGACGAGTACCTGCGAAGT-3′	NM002563	353
	5′-AGAATGGGGTCCACACAACTGTTGAG-3′		
P2Y$_2$	5′-GTGTCTGGGCGTCTTACGACCTCT-3′	NM176072	215
	5′-GCATGACTGAGCTGTAGGCCACGAA-3′		
GAPDH	5′-GAAGGTGAAGGTCGGAGTC-3′	NM002046	242
	5′-GAAGATG GTGATGGGATTTC-3′		

were separated in 1% agarose in Tris-borate buffer containing 0.25 µg per mL ethidium bromide. The gel was visualized by ultraviolet B radiation. PCR primers were designed using Genetyx Software program (GENETYX, Japan). The primers (forward, reverse, accession number, and product size) are shown in Table I.

Cell viability The applied condition of ATP for 6 h (300 µM) and the condition of 6 h post-treatment with UVB (30 and 60 mJ per cm^2) on the cytotoxicity were assessed using an AlamarBlue assay (Alamar Biosciences, Camarillo, California), according to the manufacturer's protocol. The fluorescence intensities were determined at 544 and 590 nm.

Statistics Data represent the mean ± SD. Statistical differences between two groups were determined by a two-tailed Student's test. In the case of more than two groups, differences were analyzed by analysis of variance (ANOVA test) and Scheffe's test. $p < 0.05$ was considered to be statistically significant.

Address correspondence to: Kaori Inoue, PhD, Shiseido Research Center, 2-12-1 Fukuura, Kanazawa-ku, Yokohama 236-8643, Japan. Email: kaori.inoue@to.shiseido.co.jp

References

Bo X, Jiang L-H, Wilson HL, Kim M, Burnstock G, Surprenant A, North RA: Pharmacological and biophysical properties of the human P2X$_5$ receptor. Mol Pharmacol 63:1407–1416, 2003

Burnstock G, Wood JN: Purinergic receptors: Their role in nociception and primary afferent neurotransmission. Curr Opin Neurobiol 6:526–532, 1996

Burrell HE, Bowler WB, Gallagher JA, Sharpe GR: Human keratinocytes express multiple P2Y-receptors: Evidence for functional P2Y1, P2Y2, and P2Y4 receptors. J Invest Dermatol 120:440–447, 2003

Chen CC, Akopian AN, Sivilotti L, Colquhoun D, Burnstock G, Wood JN: A P2X purinoceptor expressed by a subset of sensory neurons. Nature 377:428–431, 1995

Cook SP, McCleskey EW: Cell damage excites nociceptors through release of cytosolic ATP. Pain 95:41–47, 2002

Denda M, Inoue K, Fuziwara S, Denda S: P2X purinergic receptor antagonist accelerates skin barrier repair and prevents epidermal hyperplasia induced by skin barrier disruption. J Invest Dermatol 119:1034–1040, 2002

Dixon CJ, Bowler WB, Littlewood-Evans A, Dillon JP, Bilbe G, Sharpe GR, Gallagher JA: Regulation of epidermal homeostasis through P2Y$_2$ receptors. Br J Pharmacol 127:1680–1686, 1999

Evans RJ, Surprenant A: P2X receptors in autonomic and sensory neurons. Semin Neurosci 8:217–223, 1996

Ferguson DR, Kennedy I, Burton TJ: ATP is released from rabbit urinary bladder epithelial cells by hydrostatic pressure changes—a possible sensory mechanism? J Physiol 505:503–511, 1997

Ferrari D, Chiozzi P, Falzoni S, Dal Susino M, Collo G, Buell G, Di Virgilio F: ATP-mediated cytotoxicity in microglial cells. Neuropharmacol 36:1295–1301, 1997

Glass R, Townsend-Nichols A, Burnstock G: P2 receptors in the thymus: Expression of P2X and P2Y receptors in adult rats, an immunohistochemical and in situ hybridisation study. Cell Tissue Res 300:295–306, 2000

Greig AVH, Linge C, Terenghi G, McGrouther A, Burnstock G: Purinergic receptors are part of a functional signaling system for proliferation and differentiation of human epidermal keratinocytes. J Invest Dermatol 120:1007–1015, 2003

Grubb BD, Evans RJ: Characterization of cultured dorsal root ganglion neuron P2X receptors. Eur J Neurosci 11:149–154, 1999

Grynkiewicz G, Poenie M, Tsien RY: A new generation of Ca^{2+} indicators with greatly improved fluorescence properties. J Biol Chem 260:3440–3450, 1985

Hamill OP, Marty A, Neher E, Sakmann B, Sigworth FJ: Improved patch-clamp techniques for high-resolution current recording from cells and cell-free membrane patches. Pflugers Arch 391:85–100, 1981

Hansen M, Boitano S, Dirksen ER, Sanderson MJ: Intercellular calcium signaling induced by extracellular adenosine 5'-triphosphate and mechanical stimulation in airway epithelial cells. J Cell Sci 106:995–1004, 1993

Hennings H, Kruszewski FH, Yuspa SH, Tucker RW: Intracellular calcium alterations in response to increased external calcium in normal and neoplastic keratinocytes. Carcinogenesis 10:777–780, 1989

Jaken Y, Yuspa SH: Early signals for keratinocyte differentiation: Role of Ca^{2+}-mediated inositol lipid metabolism in normal and neoplastic epidermal cells. Carcinogenesis 9:1033–1038, 1988

Jiang L-H, Mackenzie AB, North RA, Surprenant A: Brilliant Blue G selectively blocks ATP-gated rat P2X$_7$ receptors. Mol Pharmacol 58:82–88, 2000

Koegel H, Alzheimer C: Expression and biological significance of Ca^{2+}-activated ion channels in human keratinocytes. FASEB 15:145–154, 2001

Koizumi S, Fujishita K, Inoue K, Shigemoto-Mogami Y, Tsuda M, Inoue K: Ca^{2+} waves in keratinocytes are transmitted to sensory neurons: The involvement of extracellular ATP and P2Y2 receptor activation. Biochem J 380:329–338, 2004

Koizumi S, Inoue K: Inhibition by ATP of calcium oscillations in rat cultured hippocampal neurones. Br J Pharmacol 122:51–58, 1997

Lee WK, Choi SW, Lee HR, Lee EJ, Lee KH, Kim HO: Purinoceptor-mediated calcium mobilization and proliferation in HaCaT keratinocytes. J Dermatol Sci 25:97–105, 2001

Lewis C, Neldhart S, Holy C, North RA, Buell G, Surprenant A: Coexpression of P2X$_2$ and P2X$_3$ receptor subunits can account for ATP-gated currents in sensory neurons. Nature 377:432–435, 1995

Mauro TM, Pappone PA, Isseroff RR: Extracellular calcium affects the membrane currents of cultured human keratinocytes. J Cell Physiol 143:13–20, 1990

Milner P, Bodin P, Loesch A, Burnstock G: Rapid release of endothelin and ATP from isolated aortic endothelial cells exposed to increased flow. Biochem Biophys Res Commun 170:649–656, 1990

Nakazawa K: Modulation of the inhibitory action of ATP on acetylcholine-activated current by protein phosphorylation in rat sympathetic neurons. Pflugers Arch 427:129–135, 1994

Norenberg W, Illes P: Neuronal P2X receptors: Location and functional properties. Naunyn-Schmiedeberg's Arch Pharmacol 362:324–339, 2000

North RA, Surprenant A: Pharmacology of cloned P2X receptors. Annu Rev Pharmacol Toxicol 40:563–580, 2000

Pillai S, Bikle DD: Adenosine triphosphate stimulates phosphoinositide metabolism, mobilizes intracellular calcium, and inhibits terminal differentiation of human epidermal keratinocytes. J Clin Invest 90:42–51, 1992

Schwarz A, Bhardwaj R, Aragane Y, et al: Ultraviolet-B-induced apoptosis of keratinocytes: Evidence for partial involvement of tumor necrosis factor-α in the formation of sunburn cells. J Invest Dermatol 104:922–927, 1995

Sun Y, Chai TC: Up-regulation of P2X$_3$ receptor during stretch of bladder urothelial cells from patients with interstitial cystitis. J Urol 171:448–452, 2004

Sun Y, Keay S, De Deyne PG, Chai TC: Augmented stretch activated adenosine triphosphate release from bladder uroepithelial cells in patients with interstitial cystitis. J Urol 166:1951–1956, 2001

Thorne PR, Housley GD: Purinergic signaling in sensory systems. Semin Neurosci 8:233–246, 1996

Ueno S, Koizumi S, Inoue K: Characterization of Ca^{2+} influx through recombinant P2X receptor in C6BU-1 cells. Br J Pharmacol 124:1484–1490, 1998

Thyroid Hormone Targets Matrix Gla Protein Gene Associated With Vascular Smooth Muscle Calcification

Yoji Sato, Ryo Nakamura, Mitsutoshi Satoh, Kayoko Fujishita, Satoko Mori, Seiichi Ishida,
Teruhide Yamaguchi, Kazuhide Inoue, Taku Nagao, Yasuo Ohno

Abstract—Thyroid hormones have marked cardiovascular effects in vivo. However, their direct effects on vascular smooth muscle cells have been unclear. Because thyroid hormones play critical roles in bone remodeling, we hypothesized that they are also associated with vascular smooth muscle calcification, one of the pathological features of vascular sclerosis. To test this hypothesis, we examined the effects of $3',3,5$-triiodo-L-thyronine (T_3) on the expression of calcification-associated genes in rat aortic smooth muscle cells (RAOSMCs). Quantitative RT-PCRs revealed that a physiological concentration of T_3 (15 pmol/L free T_3) increased mRNA level of matrix Gla protein (MGP), which acts as a potent inhibitor of vascular calcification in vivo, by 3-fold in RAOSMCs, as well as in cultured human coronary artery smooth muscle cells. In RAOSMCs transiently transfected with a luciferase reporter gene driven by the MGP promoter, T_3 significantly stimulated luciferase activity. In addition, RNA interference against thyroid hormone receptor-α gene diminished the effect of T_3 on MGP expression. Aortic smooth muscle tissues from methimazole-induced hypothyroid rats (400 mg/L drinking water; 4 weeks) also showed a 68% decrease in the MGP mRNA level, as well as a 33% increase in calcium content compared with that from the control euthyroid animals, whereas hyperthyroidism (0.2 mg T_3/kg IP; 10 days) upregulated MGP mRNA by 4.5-fold and reduced calcium content by 11%. Our findings suggest that a physiological concentration of thyroid hormone directly facilitates MGP gene expression in smooth muscle cells via thyroid hormone nuclear receptors, leading to prevention of vascular calcification in vivo. (*Circ Res*. 2005;97:550-557.)

Key Words: calcium ■ gene expression ■ nuclear receptors ■ vascular smooth muscle ■ thyroid hormone

Thyroid hormone has marked effects on differentiation, development, and metabolic balance of virtually every body tissue. The action of thyroid hormone is mediated by high-affinity thyroid hormone nuclear receptors (TRs), which recognize specific response elements in the promoters of target genes and regulate their transcriptional activity in response to the hormone. Alterations in thyroid hormone levels have a profound impact on the cardiovascular system, which include changes in myocardial contractility, heart rate, and resistance of peripheral vasculature. Hyperthyroidism leads to positive inotropic, lusitropic, and chronotropic effects on the heart and low systemic vascular resistance, whereas the opposite is observed in hypothyroidism. In myocardium, the mechanisms for these changes are based on altered expression levels of several key proteins involved in the regulation of intracellular ion homeostasis. The effects of thyroid hormone on cardiac contractility as well as rates of contraction and relaxation are mainly mediated by increases in the levels of the sarcoplasmic reticulum Ca^{2+}-ATPase and decreases in its inhibitor phospholamban in cardiomyocytes.[1] The positive chronotropic effect of thyroid hormone is associated with altered expression levels in plasmalemmal ion channels/transporters in the heart, such as Kv1.5, Kv4.2, minK, hyperpolarization-activated cyclic nucleotide-gated channel 2 (HCN2), HCN4, Na^+-Ca^{2+} exchanger, and Na^+-K^+-ATPase.[2–5] In contrast, although ≈25% of hypothyroid patients have diastolic hypertension,[6] the mechanism for the altered systemic vascular resistance under an abnormal thyroid hormone status is not well understood. To date, a loss of nongenomic vasodilating action of thyroid hormone[7] and atherosclerosis attributable to hypercholesterolemia[8] have been associated with the increased systemic vascular resistance under hypothyroidism.[9] Recently, mRNAs for TR isoforms were identified in aortic and coronary smooth muscle cells, suggesting that a direct genomic action of thyroid hormone may play a significant role in vascular smooth muscle.[10] Although extremely high concentrations of thyroid hormone are known to regulate expression of several genes in vascular smooth muscle cells,[10,11] the physiological and direct target genes of thyroid hormone in vascular smooth muscle cells are not known.[9]

Arterial calcification is a common pathological feature of vascular sclerosis, as well as a variety of metabolic disorders such as diabetes and renal disease. Decades ago, cretinism

was found to be associated with arterial calcification, especially when patients did not receive sufficient thyroid hormone replacement therapy.[12] However, the mechanism for the calcification in cretins has been to date unclear. A subset of vascular smooth muscle cells, named "calcifying vascular cells," was demonstrated recently to undergo osteogenic and chondrogenic differentiation in culture, indicating that some vascular smooth muscle cells still have the potential for multiple lineages.[13] Because thyroid hormone plays a critical role in bone remodeling,[14] we hypothesized that thyroid hormone is also associated with vascular calcification. To test this hypothesis, we investigated the effect of thyroid hormone on vascular smooth muscle calcification and expression profiles of calcification-associated genes in vitro and in vivo, and identified matrix Gla protein (MGP) gene as a target of thyroid hormone in vascular smooth muscle cells.

Materials and Methods

Cell Culture

α-Actin–positive rat aortic smooth muscle cells (RAOSMCs) were obtained from Cell Applications, Inc. and were cultured on 6-well cell culture plates at 37°C in a humidified atmosphere of 95% air/5% CO_2 in growth medium (GM; Dulbecco's Minimal Essential Medium [DMEM] supplemented with 10% FCS, 100 U/mL penicillin, and 100 μg/mL streptomycin). Cells up to passage 5 were used for the experiments. The culture media were changed every 48 hours. Thyroid hormone–depleted serum was prepared as described previously.[15] To evaluate effects of thyroid hormone on gene expression profiles of the synthetic phenotype of RAOSMCs, the cells at 50% of confluence were cultured in thyroid hormone–depleted medium (TDM; DMEM containing 10% thyroid hormone-depleted serum, 100 U/mL penicillin, and 100 μg/mL streptomycin) for 2 days and stimulated with 3′,3,5-triiodo-L-thyronine (T_3) for another 2 days. The contractile form of RAOSMCs was obtained by culturing confluent cells in serum-free differentiation medium (DM; DMEM supplemented with 1× ITS-X (Invitrogen), 5 mmol/L taurine, 100 U/mL penicillin, and 100 μg/mL streptomycin) for 10 days, followed by T_3 treatment for 2 days. The transition of the cell phenotype in DM was confirmed by immunoblotting for nonmuscle myosin heavy chain (SMemb) and smooth muscle myosin heavy chain-2 (SM2). To examine effects of thyroid hormone on calcium accumulation, confluent RAOSMCs were cultured as described previously[16] in TDM with or without 100 ng/mL recombinant human bone morphogenic protein-2 (rBMP2; R & D Systems) in a cell culture dish with or without collagen type IV (Col4) coating (BD Biosciences). Supplementation with β-glycerophosphate, which facilitates smooth muscle cell calcification,[17] was omitted because of a decrease in the signal-to-background ratio. Cells were subsequently stimulated with T_3 for 5 days. The concentrations of free T_3 (fT_3) and free L-thyroxine (T_4) in the serum-containing medium were determined using chemiluminescent enzyme immunoassay at a clinical diagnostic laboratory. The detection limits for fT_3 and fT_4 were 1.1 pmol/L and 1.7 pmol/L, respectively. Human coronary artery smooth muscle cells (HCASMCs; Cell Applications, Inc.) were maintained and transformed into the contractile phenotype before treatment with T_3 by culturing for 7 days in serum-free HCASMC DM (311D-500; Cell Applications, Inc) according to manufacturer instructions.

Animals

Male Sprague-Dawley rats (Japan SLC; Shizuoka, Japan) were maintained on rodent chow (Certified diet MF; Oriental Yeast, Co) and given water ad libitum. For generation of hypothyroid animals, methimazole (MMI; 400 mg/L) was added to the drinking water for 4 weeks. Hyperthyroid rats were generated by daily injection of T_3 (0.2 mg/kg body weight IP) for 10 days. Plasma concentrations of

fT_3 and fT_4 were measured, as described above. After the treatment with MMI or T_3, the thoracic aorta was isolated. Animals were 12 weeks old when killed. Aortic smooth muscle tissue for measurements of calcium accumulation and gene expression was cleared of fat, connective tissue, and an endothelium and stored at −80°C until use. For pathological examination, the aortic tissue was fixed in 10% formaldehyde. Transverse aortic sections were taken from the fixed tissue and stained with hematoxylin and eosin. All animals were treated in accordance with laboratory animal care guidelines of National Institute of Health Sciences at Tokyo.

Calcium Accumulation

Calcium content in RAOSMCs and rat aortic smooth muscle tissues were determined as described previously[16] using o-cresolphthalein complexone method. Protein concentration was determined using Bio-Rad protein assay reagent and BSA as a standard.

Real-Time Quantitative RT-PCR

Total RNA was isolated from smooth muscle cells and tissues using Sepasol reagent (Nakalai Tesque) containing 0.1 mg/mL glycogen (Roche Diagnostics) and was treated with DNaseI (Promega) according to the manufacturer protocols. To quantitate specific mRNA levels, the real-time progress of target sequence-specific amplification was monitored during RT-PCR using TaqMan chemistry and PRISM7000 Sequence Detection System (Applied Biosystems). An 18S ribosomal RNA was used as an internal control for each RNA level. Sequences of the primers and the TaqMan probes are listed in supplemental Table I (available online at http://circres.ahajournals.org).

Western Blot Analysis

RAOSMCs and aortic smooth muscle tissues were homogenized in lysis buffer as described previously.[18] After measuring protein concentrations, proteins were separated by SDS-PAGE and blotted onto polyvinylidene fluoride membranes, which were incubated with anti-SMemb or anti-SM2 monoclonal antibodies (Yamasa) or an anti-MGP polyclonal antibody (TransGenic) for 1 hour at room temperature. Subsequently, membranes were incubated with the secondary antibody conjugated with horseradish peroxidase for 1 hour. Signals were visualized and quantified using ECL Plus system (Amersham Biosciences) and LAS-3000 Imaging System (FUJIFILM), respectively.

Promoter Activity Assay

Fragments between −1752 and −1 of 5′ flanking sequence of the MGP gene exon 1 and between −1895 and −1 of 5′ flanking sequence of the stanniocalcin-1 (STC1) gene exon 1 were amplified using rat tail genomic DNA as a template. The primers for PCR amplifications were designed as based on the nucleotide sequences (MGP forward: CAAGGGTACCGGTTTGAGAGACCACGAGAC; MGP reverse: CTTGAAGCTTCCTGTGAGTCTGCCTCTGTG; STC1 forward: CAAGCTCGAGCCCCTGATATTTCAGCATGG; STC1 reverse: CTTGAAGCTTAGGTGAGGATTTGAGGAGG). The amplicons were subcloned into the firefly luciferase expression vector pGL3-Basic (Promega). RAOSMCs in the contractile state, grown on a 24-well plate, were transiently cotransfected with 225 ng/well of each promoter luciferase plasmid and 75 ng/well of phRL-TK control plasmid (Promega) using FuGene6 (Roche). Three hours after transfection, cells were incubated with or without T_3. The luciferase activity was defined as a ratio of the firefly luciferase signal to the renilla luciferase signal, which was measured with Dual-Luciferase Reagent (Promega). The transfection efficiency of the plasmids was estimated to be 1% to 10% of the total RAOSMCs, as assessed by transfection experiments with an enhanced green fluorescent protein expression vector pEGFP-N1 (BD Biosciences Clontech; data not shown).

RNA Interference Against TRα

RAOSMCs in the synthetic form were transiently transfected with StealthRNAi (Invitrogen) specific for TRα gene (sense: CCAGAAGAACCUCCAUCCCACCUAU; antisense: AUAGGUGGGAUG-

Free Thyroid Hormone Concentrations in Rat Plasma and Serum-Containing Cell Culture Medium

Plasma/Medium	fT_3 (pmol/L)	fT_4 (pmol/L)	Calculated Range of Thyroid Hormone Activity (pmol fT_3/L)
Plasma from a euthyroid rat	4.2 ± 0.6	27 ± 2	6.9–31
Plasma from a hypothyroid rat (MMI treatment for 1 month)	<1.1	<1.8	<1.3–2.9
GM (DMEM, 10% FCS, P/S)	3.7 ± 0.2	15 ± 0.0	5.2–19
TDM (DMEM, 10% thyroid hormone–depleted FCS, P/S)	<1.1	2.7 ± 0.2	<1.4–3.8
TDM (DMEM, 10% thyroid hormone–depleted FCS, P/S) + 1 nmol/L T_3	$15 \pm 1^*$	$3.4 \pm 0.1^*$	15–18

The range of thyroid hormone activity was calculated assuming that X% (X=0–100) of T_4 is processed to T_3 at the site of action in vivo and that the affinity of T_4 for TRs is one tenth that of T_3.

P/S indicates penicillin and streptomycin.

Values are means ± SD; *$P < 0.05$ vs TDM without T_3 supplementation (Student t test).

GAGGUUCUUCUGG) or StealthRNAi negative control medium GC (Invitrogen) using Lipofectamine 2000 (Invitrogen), according to manufacturer instructions and incubated in TDM for 2 days. Cells were then treated with or without T_3 (15 pmol/L fT_3) for another 2 days. Total RNA was isolated from cells before and after T_3 treatment for mRNA determinations.

Statistics

Data were expressed as means ± SEM unless otherwise indicated. Data were analyzed for statistical significance by Student t test or ANOVA with Student-Newman–Keuls test as a post hoc test. Significance was imparted at the $P < 0.05$ level.

Results

Free Thyroid Hormone Concentrations

As shown in the Table, plasma concentrations of fT_3 and fT_4 in euthyroid rats were 4.2 ± 0.6 pmol/L and 27 ± 2 pmol/L (mean ± SD), respectively. The MMI treatment decreased fT_3 and fT_4 to <1.1 pmol/L and to <1.8 pmol/L, respectively, indicating that the animals were hypothyroid. The fT_3 and fT_4 levels in GM containing 10% FCS were 3.7 ± 0.2 pmol/L and 15 ± 0.0 pmol/L (mean ± SD), respectively, and happened to be similar to those in plasma from euthyroid rats. The free concentrations of thyroid hormones in TDM (<1.1 pmol/L fT_3; 2.7 pmol/L fT_4) were low enough to keep TRs inactivated because the K_d values of T_3 for TRs are known to be ≈ 10 to 100 pmol/L[19] and because T_4 has ≈ 10-fold lower affinity for TRs than that of T_3. In vascular smooth muscle cells, T_4 is known to be converted to T_3 by type II iodothyronine deiodinase,[10] although the conversion rate in vivo is not clear. Assuming that X% (X=0 to 100) of T_4 is processed to T_3 at the site of action in vivo and that the affinity of T_4 for TRs is one tenth of that of T_3, the total activity of thyroid hormones in euthyroid rat plasma should be equivalent to that of 6.9 to 31 pmol/L $[4.2 + 27 \times X/100 + 27 \times (1 - X/100)/10]$ of fT_3 alone. The supplementation of T_3 to TDM at 1 nmol/L of total concentration resulted in an increase in fT_3 to 15 ± 1 pmol/L (mean ± SD), with a slight increase in fT_4, therefore, it was regarded within a euthyroid range.

T_3-Induced Gene Expression and Calcification in Cultured RAOSMCs

Vascular smooth muscle cells show a high degree of plasticity and are able to interchange between a differentiated, contractile phenotype and a proliferating, synthetic phenotype. Therefore, we first examined the effects of T_3 on expression profiles of calcification-associated genes in both phenotypes. RAOSMCs in GM predominantly expressed a marker of synthetic phenotype: SMemb. The replacement of the medium with DM reduced the protein level of SMemb to 28% and increased SM2 expression by 11.6-fold (online Figure I), indicating the transition of the phenotype. In the synthetic phenotype, T_3 (1 nmol/L total T_3=15 pmol/L fT_3) led to upregulation of mRNAs for MGP and STC1×3.3-fold and 1.3-fold, respectively (Figure 1A), whereas osteopontin
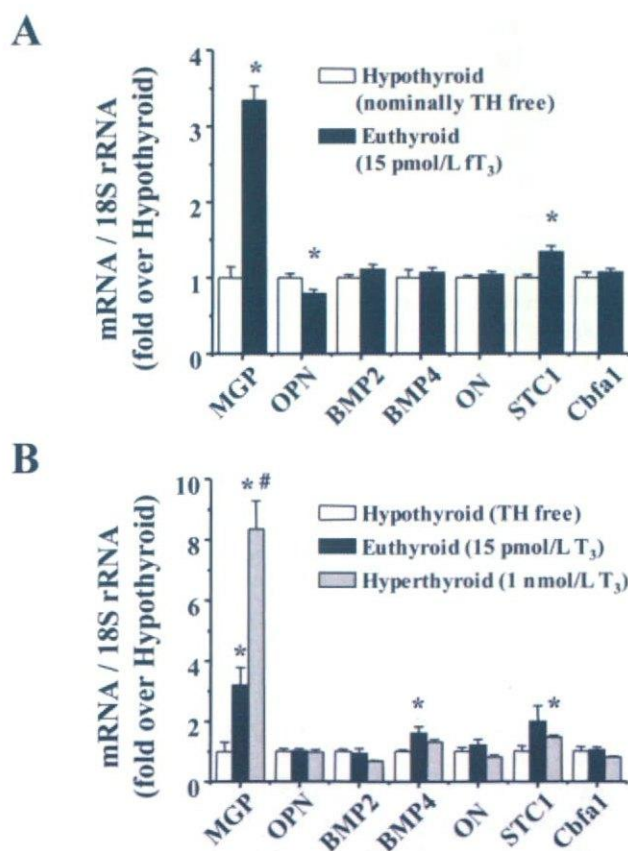
Figure 1. T_3 regulated expression of calcification-associated genes in cultured RAOSMCs in synthetic and contractile forms. A, Effect of T_3 on mRNA expression of calcification-associated genes in the synthetic form of RAOSMCs cultured in TDM. Cells were treated with 15 pmol/L fT_3 for 2 days. B, Effect of T_3 on mRNA expression of calcification-associated genes in the contractile form of RAOSMCs cultured in the DM. Cells were treated with 15 pmol/L or 1 nmol/L T_3 for 2 days. Values are expressed as means ± SEM (n=4) TH indicates thyroid hormone. *$P < 0.05$ vs hypothyroid; #$P < 0.05$ vs euthyroid.
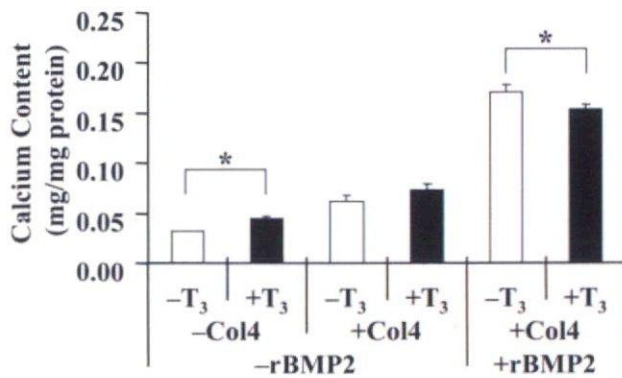
Figure 2. Effects of T_3 on calcium accumulation in cultured RAOSMCs. The confluent cells cultured in TDM were stimulated by 15 pmol/L fT_3. In the absence of rBMP2, T_3 significantly increased calcium content in RAOSMCs cultured in noncoated vessels. Supplementation with rBMP2 increased the basal calcium content in RAOSMCs in Col4-coated vessels and reversed the effect of T_3 on the calcification. Values are expressed as means$\pm$SEM (n=6 to 8); *$P<0.05$.

(OPN) was downregulated by 21%. The mRNA levels of BMP2, bone morphogenic protein-4 (BMP4), osteonectin (ON), and core binding factor $\alpha1$ (Cbfa1; also known as Runx2 or Osf2) were not significantly altered by the T_3 treatment. Specific signals for osteocalcin and bone sialoprotein mRNA were not detected by several independent primer sets in all experiments of the present study, presumably because of their low abundance in vascular smooth muscle cells. In the contractile phenotype in DM, T_3 (15 pmol/L) induced upregulation of MGP and BMP4$\times$3.2-fold and 1.6-fold, respectively (Figure 1B). A higher concentration of T_3 (1 nmol/L) resulted in a further increase in the MGP mRNA level and a significant upregulation of STC1 mRNA, indicating the dose dependency of the effects. Messenger RNA levels of OPN, BMP2, ON, STC1, and Cbfa1 in the contractile phenotype were not significantly altered by the T_3 treatment. Among the calcification-associated genes, MGP and STC1 genes were commonly upregulated by T_3 in both phenotypes, suggesting that these two genes were relatively essential in RAOSMCs as targets of thyroid hormone.

Because the effect of MGP on calcification and osteogenic differentiation of vascular smooth muscle cells depends on availability of BMP2 and Col4,[20,21] cell calcification was determined in the absence or presence of these factors. In the absence of rBMP2 and Col4 coating, treatment with T_3 (1 nmol/L total T_3=15 pmol/L fT_3) for 5 days resulted in an increase in calcium content by 39% in RAOSMCs (Figure 2). The same treatment tended to have the similar effect on cells in a Col4-coated vessel in the absence of rBMP2. In contrast, T_3 led to a significant decrease in cellular calcium by 10% in the presence of rBMP2 and Col4-coating.

Transcriptional Regulation of MGP and STC1 Genes by T_3

To test a hypothesis that the promoters of MGP and STC1 genes were under regulation of thyroid hormone, RAOSMCs were transiently transfected with luciferase reporters under control of the MGP and STC1 promoters. The 5′ flanking sequences of MGP and STC1 genes have been submitted to
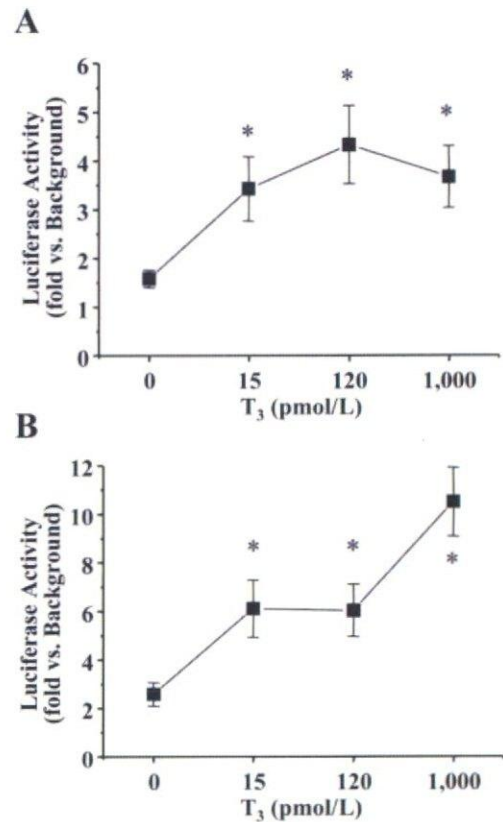
Figure 3. T_3 activated luciferase reporter genes driven by rat MGP (A) and STC1 (B) promoters in the contractile form of RAOSMCs. Cells were transiently cotransfected with a reporter plasmid containing a promoter region of rat MGP or STC1 gene and an internal control plasmid (phRL-tk) and were treated with T_3 for 2 days. The cell extracts were assayed for luciferase activity. Values are normalized to the background (luciferase activity of the cells transfected with promoterless pGL3-Basic vector and phRL-tk) and expressed as means$\pm$SEM (n=6); *$P<0.05$ vs control.

NCBI (accession numbers AY750958 and AY750959, respectively). Transcription Element Search System (TESS)[22] revealed that consensus sequences of the thyroid hormone response element were located in 585 to 600 (*TGTAC-CCCAATGAACC*) and 1009 to 1024 (*TGGAGACAGGAG-GACA*) bases upstream of the putative transcription initiation sites of MGP and STC1 genes, respectively. Treatments of the cells with T_3 (15 pmol/L to 1 nmol/L) for 48 hours resulted in significant increases in transcriptional activity compared with vehicle treatment (Figure 3).

Regulation of MGP and STC1 Expression via TRs

Arterial smooth muscle cells express $TR\alpha1$ and $TR\alpha2$ nuclear receptor isoforms strongly and $TR\beta1$ and $TR\beta2$ relatively weakly.[10] To evaluate the involvement of TRs in the T_3-induced upregulation of MGP and STC1 mRNAs, RNA interference (RNAi) was performed using StealthRNAi specific for the $TR\alpha$ gene encoding $TR\alpha1$ and $TR\alpha2$. The RNAi in RAOSMCs for 2 days significantly attenuated mRNA expression of $TR\alpha1$ and $TR\alpha2$ by 66% and 57%, respectively, compared with the controls (Figure 4). The RNAi was also associated with upregulation of MGP mRNA by 32%
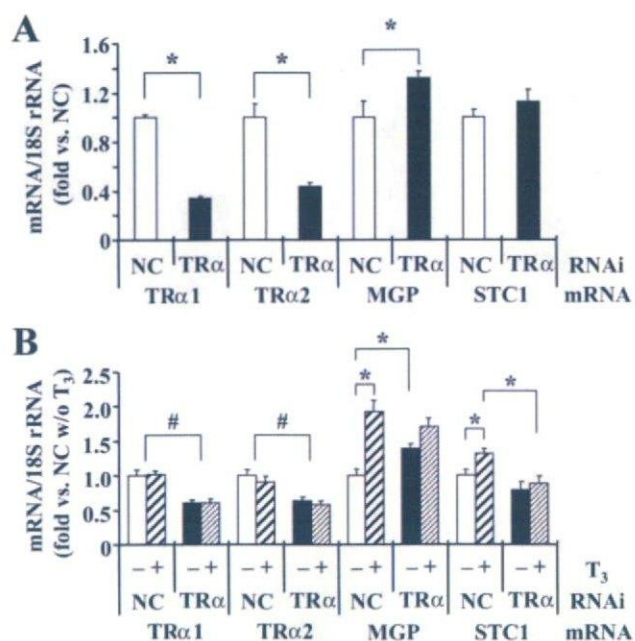
Figure 4. The RNAi against TRα gene in RAOSMCs (synthetic form). A, RNAi against TRα gene for 2 days led to significant decreases in expression of TRα1 and TRα2 to the same extent and a slight increase in the MGP expression. B, The expression of TRα1 and TRα2 remained reduced after the following incubation for 2 more days and was not altered by T$_3$ (15 pmol/L fT$_3$). The RNAi was associated with loss of responsiveness of MGP and STC1 mRNA to T$_3$. Values are expressed as means$\pm$SEM (n=4 to 6 [A] and 8 [B]). NC indicates negative control. *$P<0.05$ (Student t test [A] or Student-Newman–Keuls test [B]); #$P<0.05$ association with RNAi (two-way ANOVA).

compared with the controls, suggesting that unliganded TRα1 or TRα2, which has no affinity for thyroid hormones, had an inhibitory effect on the expression of MGP. The mRNA level of STC1 was not altered by the RNAi. Incubation with 15 pmol/L fT$_3$ for the following 2 days facilitated the expression of MGP and STC1 in the control group, whereas no significant effect of T$_3$ on MGP and STC1 gene expression was detected in the RNAi group. T$_3$ had no effect on the expression of the TRα isoforms.

Calcium Accumulation in Hypothyroid Rat Aorta

As examined by hematoxylin-eosin staining, the cross-sections of aorta from rats treated with MMI for 4 weeks did not show obvious calcified foci (Figure 5A). However, *o*-cresolphthalein complexone experiments indicated that the 4-week treatment with MMI significantly increased the calcium content in the rat aortic smooth muscle tissues by 33% compared with that of euthyroid animals (Figure 5B). Quantitative RT-PCRs revealed that mRNA levels of MGP, BMP4, ON, and Cbfa1 were downregulated by 68%, 87%, 69%, and 72%, respectively, by the MMI treatment. OPN, BMP2, and STC1 mRNA levels were not significantly altered (Figure 5C). MMI also attenuated protein expression of MGP by 54% (Figure 5D). Calcified foci were not observed even in aortic cross-sections from rats treated with MMI for 12 weeks (online Figure II), suggesting that the calcification was not progressive.

Calcium Content in Hyperthyroid Rat Aorta

Hyperthyroidism elicits pronounced vascular relaxation.[9] However, the effect of hyperthyroidism on vascular calcification has been unclear. Therefore, it is of interest to compare effects of hyperthyroidism on the expression profiles of calcification-associated genes with those of hypothyroidism. In contrast to the aortic smooth muscle from hypothyroid rats, daily injections of T$_3$ for 10 days led to a decrease in the calcium content in the rat aortic smooth muscle tissues by 11% compared with that of euthyroid animals (Figure 6A). Quantitative RT-PCRs showed that mRNA levels of MGP, OPN, and BMP2 were upregulated by 4.5-fold, 4.9-fold, and 3.4-fold, respectively, by the T$_3$ treatment, whereas hyperthyroidism resulted in a significant decrease in the level of STC1 mRNA (Figure 6B).

Upregulation of MGP mRNA in Cultured HCASMCs

To demonstrate that thyroid hormone regulates MGP gene expression in vascular smooth muscle cells of a different species, we determined MGP mRNA levels in HCASMCs in the presence and absence of T$_3$. Treatment with a physiological concentration (15 pmol/L) of T$_3$ for 2 days led to a significant increase in MGP mRNA by 40% (1.0$\pm$0.07 [hypothyroid 0 pmol/L T$_3$] versus 1.40$\pm$0.13 [euthyroid 15 pmol/L T$_3$] in an arbitrary unit; n=12).

Discussion

In the present study, thyroid hormone led to an upregulation of MGP in arterial smooth muscle cells in vitro regardless of culture condition, phenotype, and animal species of the cells. The transcriptional activity of the MGP gene was increased by T$_3$, and reduction of TRα gene expression led to a loss of responsiveness of the MGP gene to T$_3$, suggesting that the effect of T$_3$ is based on a genomic action via TRα1. Furthermore, in vivo hormone levels were positively and negatively associated with the expression of MGP and calcification in vascular smooth muscle, respectively. Because aortic smooth muscle from hypothyroid rats showed no obvious neointimal formation, the vascular calcification under the hypothyroidism is likely to be similar to that of media sclerosis. In aortic smooth muscle from hypothyroid rats, expression levels of calcification activators BMP4, ON, and Cbfa1 were decreased, whereas hyperthyroidism upregulated another calcification activator BMP2. However, calcium content in aortic smooth muscle was increased in hypothyroidism, and the opposite was observed in hyperthyroidism, suggesting that the expression or function of calcification inhibitors, such as MGP and OPN, are more dominant for the phenotypic outcome in vivo, compared with those of the calcification activators.

MGP is a mineral-binding extracellular matrix protein synthesized by vascular smooth muscle cells and chondrocytes. Luo et al have shown that ablation of MGP gene in mice causes extensive and lethal calcification and cartilaginous metaplasia of the media of all elastic arteries, indicating that MGP has an inhibitory effect on media calcification in vivo.[23] In contrast, in the same study, morphological analysis showed that heterozygous MGP knockout mice, which had a
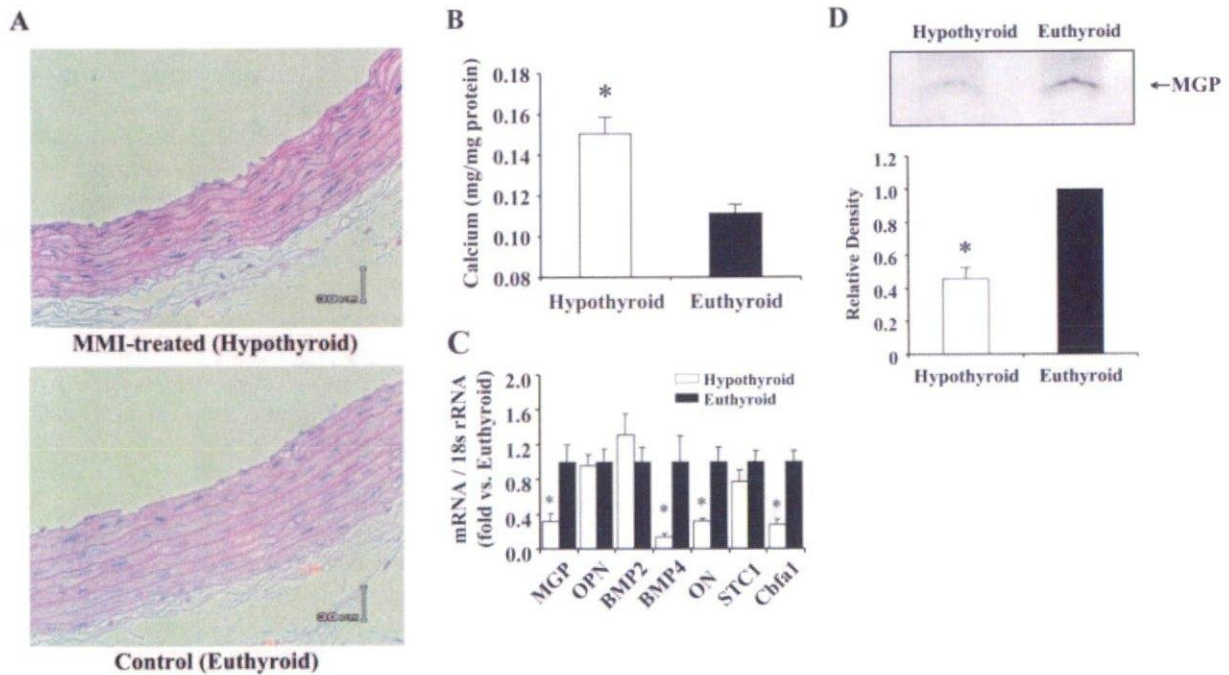
Figure 5. Hypothyroidism led to calcium accumulation in aortic smooth muscle and an altered expression profile of calcification-associated genes. Hypothyroidism was achieved by treatment of the animals with MMI (400 mg/L drinking water) for 4 weeks. A, Hematoxylin-eosin staining of cross-sections of aortae from euthyroid and hypothyroid rats. No obvious calcified foci were observed in either section. Bar=30 μm. B, Effect of the hypothyroidism on calcium deposition in rat aortic smooth muscle. C, Effect of hypothyroidism on mRNA expression of calcification-associated genes in rat aortic smooth muscle. D, Effect of hypothyroidism on MGP protein expression in rat aortic smooth muscle. Values are expressed as means±SEM (n=7 to 8); *$P<0.05$ vs euthyroid.

similar decrease in an arterial MGP level to that by the MMI treatment in the present study, had no obvious calcified foci in arterial smooth muscle. However, this does not necessarily imply that the heterozygous ablation of MGP gene does not affect calcium content in arteries because biochemical quantification for tissue calcium has not been performed. Thus, it is still possible that there is a dose-response relationship between MGP and media calcification, and that an ≈50% reduction of MGP results in some increase in calcium content, although it may not be morphologically evident.

The extracellular environment around smooth muscle cells is known to determine a functional role of MGP. Namely, calcification of vascular smooth muscle cells in the presence of a relatively high concentration of BMP2 was inhibited by MGP, whereas calcification of vascular smooth muscle cells under a low concentration of BMP2 was stimulated by MGP.[20] Moreover, extracellular matrix proteins, especially Col4, have significant influence on MGP function and vascular calcification.[21] In fact, the effect of T$_3$ on calcification of RAOSMCs was determined by these environmental factors. Therefore, these results suggest that T$_3$ regulates smooth muscle cell calcification, at least partly, by promoting MGP expression, although not only vascular cells but also migratory adventitial pericytic myofibroblasts and circulating skeletal progenitors may have some additional contributions to vascular calcification in vivo.[24]

STC1 is a mammalian homolog of stanniocalcin, the fish calcium/phosphate- regulating polypeptide that inhibits calcium flux into cells and stimulates phosphate reabsorption. In the present study, gene transcription of STC1 appeared to be

regulated by T$_3$ via TRα in a dose-dependent manner. However, the highest mRNA expression of STC1 tended to be achieved at a euthyroid status in vitro and in vivo, and hyperthyroidism significantly attenuated the STC1 mRNA expression in vivo. Recently, STC1 was shown to accelerate osteoblast development in an autocrine/paracrine manner in cultured fetal rat calvaria cells.[25] Therefore, the downregulation of STC1 may also contribute to the low calcium content in aortic smooth muscle of hyperthyroid rats, although the mechanism that offsets the increase in the STC1 gene transcription remains to be elucidated.

OPN is known to inhibit or promote vascular smooth muscle calcification in vivo in a phosphorylation-dependent manner.[26] Therefore, the changes in its expression in the synthetic form of RAOSMCs and in smooth muscle tissue of hyperthyroid rats may be also associated with the effect of thyroid hormone on calcium accumulation. However, as shown in the in vitro and MMI experiments, a physiological concentration of thyroid hormone is unlikely to target OPN gene directly, at least in the contractile form of aortic smooth muscle cells.

BMP2 was upregulated by hyperthyroidism in vivo, whereas BMP4 was downregulated by MMI-induced hypothyroidism. BMP2 is know to antagonize the effect of MGP,[20] and BMP4 has been suggested to play a significant role as a cytokine, a growth factor or a media-calcification promoter in vascular lesions of calciphylaxis.[27] The mRNA levels of ON and Cbfa1 were also decreased in hypothyroid rat aortic smooth muscle. With the exception of BMP4, these changes in vivo did not follow on from the in vitro experiments,
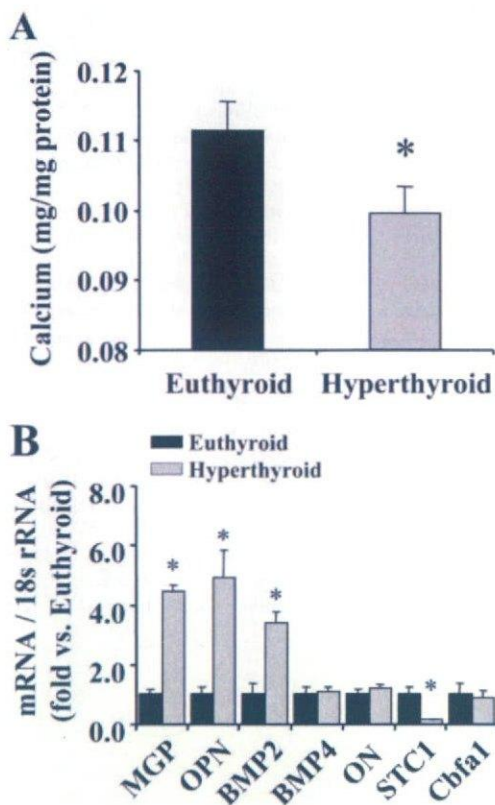
Figure 6. Hyperthyroidism decreased tissue calcium content in aortic smooth muscle and altered the expression profile of calcification-associated genes. Hyperthyroidism was achieved by daily injection of T_3 (0.2 mg/kg body weight IP) for 10 days. A, Effect of the hyperthyroidism on calcium deposition in rat aortic smooth muscle. C, Effect of hyperthyroidism on mRNA expression of calcification-associated genes in rat aortic smooth muscle. Values are expressed as means±SEM (n=7 to 8); *$P<0.05$ vs euthyroid.

cular resistance observed in hypothyroidism. Vascular calcification can lead to some other serious problems, including vascular stenosis, calciphylaxis, and even sudden death. Recently, a polymorphism in the promoter region of MGP gene was found to have a significant association with myocardial infarction in low-risk individuals and femoral calcification in the presence of atherosclerotic plaques, suggesting involvement of this mutation in coronary artery disease.[28] In addition, a recent meta-analysis of coronary artery calcium scores suggested that the calcium score is an independent risk factor to predict coronary heart disease events.[29] Therefore, further studies on the protective role of thyroid hormone and MGP against vascular smooth muscle calcification should provide insights into novel therapeutic strategies for the high systemic vascular resistance and blood pressure of hypothyroid patients, as well as for diseases associated with cardiovascular calcification such as diabetes, chronic renal insufficiency, and hypercholesterolemia.
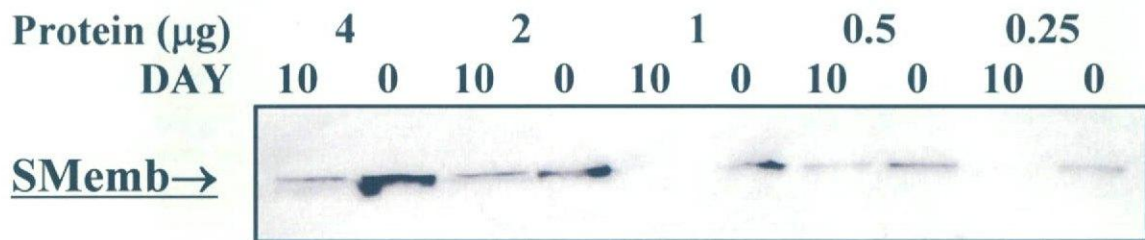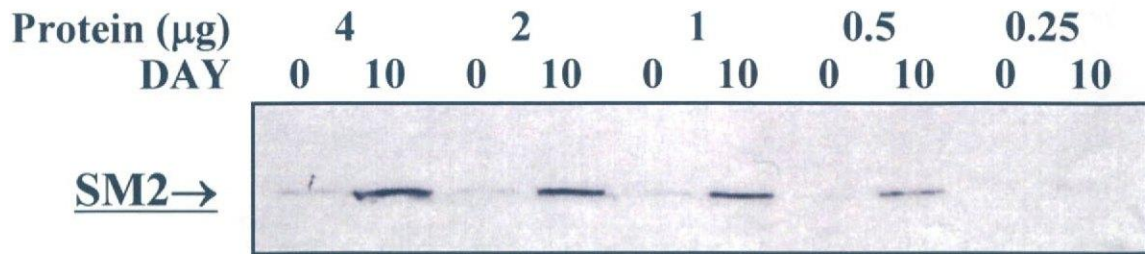
References

1. Carr AN, Kranias EG. Thyroid hormone regulation of calcium cycling proteins. *Thyroid.* 2002;12:453–457.
2. Abe A, Yamamoto T, Isome M, Ma M, Yaoita E, Kawasaki K, Kihara I, Aizawa Y. Thyroid hormone regulates expression of shaker-related potassium channel mRNA in rat heart. *Biochem Biophys Res Commun.* 1998;245:226–230.
3. Gloss B, Trost S, Bluhm W, Swanson E, Clark R, Winkfein R, Janzen K, Giles W, Chassande O, Samarut J, Dillmann W. Cardiac ion channel expression and contractile function in mice with deletion of thyroid hormone receptor alpha or beta. *Endocrinology.* 2001;142:544–550.
4. Boerth SR, Artman M. Thyroid hormone regulates Na⁻-Ca²⁺ exchanger expression during postnatal maturation and in adult rabbit ventricular myocardium. *Cardiovasc Res.* 1996;31:E145–E152.
5. Orlowski J, Lingrel JB. Thyroid and glucocorticoid hormones regulate the expression of multiple Na,K-ATPase genes in cultured neonatal rat cardiac myocytes. *J Biol Chem.* 1990;265:3462–3470.
6. Klein I, Ojamaa K. Thyroid hormone and the cardiovascular system. *N Engl J Med.* 2001;344:501–509.
7. Ojamaa K, Klemperer JD, Klein I. Acute effects of thyroid hormone on vascular smooth muscle. *Thyroid.* 1996;6:505–512.
8. Hak AE, Pols HAP, Visser TJ, Drexhage HA, Hofman A, Witteman JC. Subclinical hypothyroidism is an independent risk factor for atherosclerosis and myocardial infarction in elderly women: the Rotterdam Study. *Ann Intern Med.* 2000;132:270–278.
9. Klein I, Ojamaa K. Thyroid hormone: targeting the vascular smooth muscle cell. *Circ Res.* 2001;88:260–261.
10. Mizuma H, Murakami M, Mori M. Thyroid hormone activation in human vascular smooth muscle cells: expression of type II iodothyronine deiodinase. *Circ Res.* 2001;88:313–318.
11. Fukuyama K, Ichiki T, Takeda K, Tokunou T, Iino N, Masuda S, Ishibashi M, Egashira K, Shimokawa H, Hirano K, Kanaide H, Takeshita A. Downregulation of vascular angiotensin II type 1 receptor by thyroid hormone. *Hypertension.* 2003;41:598–603.
12. Komar NN, Gabrielsen TO. Arterial calcification in adult cretins. *Am J Roentgenol Radium Ther Nucl Med.* 1967;101:202–203.
13. Tintut Y, Alfonso Z, Saini T, Radcliff K, Watson K, Bostrom K, Demer LL. Multilineage potential of cells from the artery wall. *Circulation.* 2003;108:2505–2510.

suggesting that the alterations were not attributable to a direct effect of thyroid hormone on vascular smooth muscle cells. Because physiological concentrations of thyroid hormones upregulated BMP4 in the contractile form of RAOSMCs and in vivo (hypothyroid versus euthyroid), BMP4 may be another direct target of thyroid hormone in aortic smooth muscle cells. However, the expected influences of the changes in all the calcification activators above were apparently masked, aforementioned, indicating their minor roles in vascular calcification, compared with those of calcification inhibitors.

In summary, our findings, for the first time, demonstrate that a physiological concentration of thyroid hormone has significant genomic effects on vascular smooth muscle cells in vitro and in vivo, which are associated with vascular calcification. Most notably, a decrease in thyroid hormone and the concomitant increase in vascular calcification in vivo are marked by a decrease in the level of MGP expression, suggesting that a physiological concentration of thyroid hormone has a direct protective role against vascular smooth muscle calcification in vivo. Although vascular calcification has been thought to be benign, arterial calcification should alter vascular compliance. Thus, it is possible that the increased vascular stiffness underlies the high systemic vas-

14. Bassett JH, Williams GR. The molecular actions of thyroid hormone in bone. *Trends Endocrinol Metab*. 2003;14:356–364.

15. Samuels HH, Stanley F, Casanova J. Depletion of L-3,5,3′-triiodothyronine and L-thyroxine in euthyroid calf serum for use in cell culture studies of the action of thyroid hormone. *Endocrinology*. 1979; 105:80–85.

16. Jono S, Nishizawa Y, Shioi A, Morii H. Parathyroid hormone-related peptide as a local regulator of vascular calcification. Its inhibitory action on in vitro calcification by bovine vascular smooth muscle cells. *Arterioscler Thromb Vasc Biol*. 1997;17:1135–1142.

17. Shioi A, Nishizawa Y, Jono S, Koyama H, Hosoi M, Morii H. Beta-glycerophosphate accelerates calcification in cultured bovine vascular smooth muscle cells. *Arterioscler Thromb Vasc Biol*. 1995;15: 2003–2009.

18. Sato Y, Ferguson DG, Sako H, Dorn GW II, Kadambi VJ, Yatani A, Hoit BD, Walsh RA, Kranias EG. Cardiac-specific overexpression of mouse cardiac calsequestrin is associated with depressed cardiovascular function and hypertrophy in transgenic mice. *J Biol Chem*. 1998;273:28470–28477.

19. Lazar MA, Chin WW. Nuclear thyroid hormone receptors. *J Clin Invest*. 1990;86:1777–1782.

20. Zebboudj AF, Shin V, Bostrom K. Matrix GLA protein and BMP-2 regulate osteoinduction in calcifying vascular cells. *J Cell Biochem*. 2003;90:756–765.

21. Shin V, Zebboudj AF, Bostrom K. Endothelial cells modulate osteogenesis in calcifying vascular cells. *J Vasc Res*. 2004;41:193–201.

22. Schug J, Overton GC. TESS: Transcription Element Search Software on the WWW. In: *Technical Report CBIL-TR-1997–1001-v0.0*, Computa-tional Biology and Informatics Laboratory, School of Medicine, University of Pennsylvania, 1997:1–10.

23. Luo G, Ducy P, McKee MD, Pinero GJ, Loyer E, Behringer RR, Karsenty G. Spontaneous calcification of arteries and cartilage in mice lacking matrix GLA protein. *Nature*. 1997;386:78–81.

24. Vattikuti R, Towler DA. Osteogenic regulation of vascular calcification: an early perspective. *Am J Physiol Endocrinol Metab*. 2004;286: E686–E696.

25. Yoshiko Y, Maeda N, Aubin JE. Stanniocalcin 1 stimulates osteoblast differentiation in rat calvaria cell cultures. *Endocrinology*. 2003;144: 4134–4143.

26. Jono S, Peinado C, Giachelli CM. Phosphorylation of osteopontin is required for inhibition of vascular smooth muscle cell calcification. *J Biol Chem*. 2000;275:20197–20203.

27. Griethe W, Schmitt R, Jurgensen JS, Bachmann S, Eckardt KU, Schindler R. Bone morphogenic protein-4 expression in vascular lesions of calciphylaxis. *J Nephrol*. 2003;16:728–732.

28. Herrmann SM, Whatling C, Brand E, Nicaud V, Gariepy J, Simon A, Evans A, Ruidavets JB, Arveiler D, Luc G, Tiret L, Henney A, Cambien F. Polymorphisms of the human matrix gla protein (MGP) gene, vascular calcification, and myocardial infarction. *Arterioscler Thromb Vasc Biol*. 2000;20:2386–2393.

29. Pletcher MJ, Tice JA, Pignone M, Browner WS. Using the coronary artery calcium score to predict coronary heart disease events. A systematic review and meta-analysis. *Arch Intern Med*. 2004;164: 1285–1292.

Protein (μg)	4		2		1		0.5		0.25	
DAY	0	10	0	10	0	10	0	10	0	10

SM2→

Protein (μg)	4		2		1		0.5		0.25	
DAY	10	0	10	0	10	0	10	0	10	0

SMemb→

Representative images of immunoblots for SM2 (smooth muscle myosin heavy chain-2) and SMemb (nonmuscle myosin heavy chain) in RAOSMCs before and after treatment with the differentiation medium for 10 days. The differentiation medium altered the protein expression of SM2 and SMemb by 11.6 ± 2.8 fold (n=5) and 0.28 ± 0.04 fold (n=4), respectively.

MMI-treated (Hypothyroid)
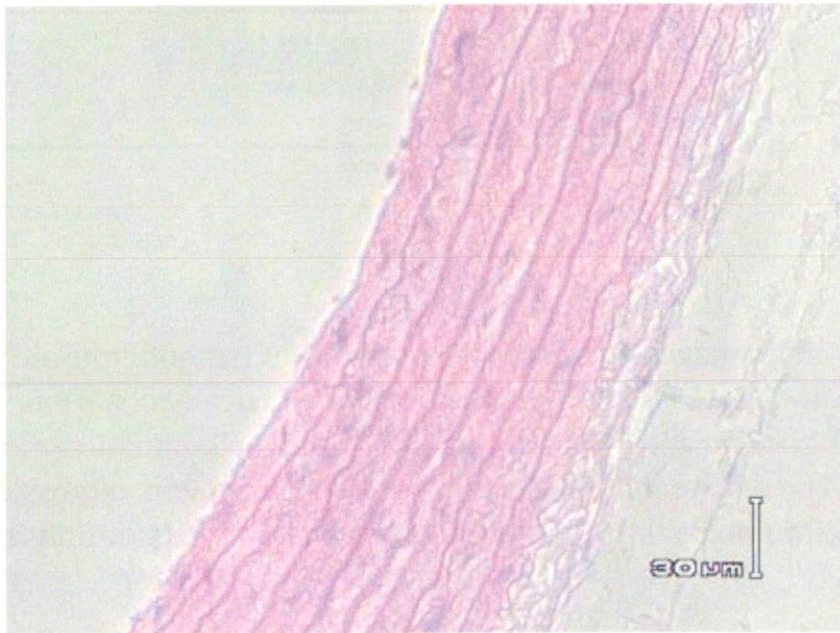
Control (Euthyroid)

Hematoxylin-Eosin staining of cross sections of aortas from a hypothyroid rat treated with methimazole (MMI, 400 mg/L drinking water) for 12 weeks and a euthyroid control rat. Bar=30μm.

Suplement Table 1. Sequences of Oligonucleotides for Quantitative RT-PCRs

BMP2:	forward primer:	5'-TGAACACAGCTGGTCTCAGGTAA-3'
	reverse primer:	5'-TGTGTTTGGCTTGACGCTTT-3'
	TaqMan probe:	5'-AGTGACTTTTGGCCACGACGGTAAAGG-3'
BMP4:	forward primer:	5'-TCAGCAGCATCCCAGAGAATG-3'
	reverse primer:	5'-TTATACGGTGGAAGCCCTGTTC-3'
	TaqMan probe:	5'-TCTGCAGAGCTCCGGCTATTTCGG-3'
Cbfa1:	forward primer:	5'-GTCTTCACAAATCCTCCCCAAGT-3'
	reverse primer:	5'-GAGGCGGTCAGAGAACAAACTAG-3'
	TaqMan probe:	5'-TATTAAAGTGACAGTGGACGGTCCCCGG-3'
MGP (rat):	forward primer:	5'-CGGAGAAATGCCAACACCTT-3'
	reverse primer:	5'-CGCTCACACAGCTTGTAGTCATC-3'
	TaqMan probe:	5'-ATGGCACGCTAAAGCCCAGGAAAGA-3'
MGP (human):	forward primer:	5'-TTCATATCCCCTCAGCAGAGATG-3'
	reverse primer:	5'-GCGATTATAGGCAGCATTGTATCC-3'
	TaqMan probe:	5'-AACGCTCTAAGCCTGTCCACGAGCTCAATA-3'
ON:	forward primer:	5'-CACCTGGACTACATCGGACCAT-3'
	reverse primer:	5'-TTGTTGCCCTCATCTCTCTCGTA-3'
	TaqMan probe:	5'-CGTGACTGGCTCAAAAACGTCCTGGT-3'
OPN:	forward primer:	5'-TGACCACATGGACGATGATGA-3'
	reverse primer:	5'-GCTTGTGTGCTGGCAGTGA-3'
	TaqMan probe:	5'-ACGGAGACCATGCAGAGAGCGAGGAT-3'
STC1:	forward primer:	5'-GGATCACCTCCAAGGTCTTCCT-3'
	reverse primer:	5'-GGCAATGCTGCAAACATTGA-3'
	TaqMan probe:	5'-TTCGGAGGTGTTCTACTTTCCAGAGGATGA-3'
TRα1	forward primer:	5'-AGCTGCTGATGAAGGTGACTGA-3'
	reverse primer:	5'-GCTTAGACTTCCTGATCCTCAAAGAC-3'
	TaqMan probe:	5'- TCCACATGAAAGTCGAGTGCCCCA-3'
TRα2	forward primer:	5'-GGCAATACCTTGTCCCTTTGAG-3'
	reverse primer:	5'-CCACGTAAGCACAGACAACTATTTC-3'
	TaqMan probe:	5'-ACTCAAGTGTCACCTCCTTCCCCAGCTC-3'

Riccardin C: A natural product that functions as a liver X receptor (LXR)α agonist and an LXRβ antagonist

Norimasa Tamehiro[a], Yoji Sato[a], Takuo Suzuki[a], Toshihiro Hashimoto[b], Yoshinori Asakawa[b], Shinji Yokoyama[c], Tohru Kawanishi[a], Yasuo Ohno[a], Kazuhide Inoue[a], Taku Nagao[a], Tomoko Nishimaki-Mogami[a,*]

[a] National Institute of Health Sciences, Kamiyoga 1-18-1, Setagaya-ku, Tokyo 158-8501, Japan
[b] Faculty of Pharmaceutical Sciences, Tokushima Bunri University, Tokushima, Japan
[c] Biochemistry, Cell Biology and Metabolism, Nagoya City University Graduate School of Medical Sciences, Nagoya, Japan

Abstract Liver X receptors (LXRs) α and β share considerable sequence homology and several functions, respond to the same endogenous and synthetic ligands, and play critical roles in maintaining lipid homeostasis. In this study, liverwort-derived riccardin C (RC) and F (RF) were identified as an LXRα agonist/LXRβ antagonist and an LXRα antagonist, respectively. RC and RF bound to LXRs, but had different abilities to recruit a coactivator and thereby induce transactivation. Despite its unique subtype-selective activity, RC enhanced ABCA1 and ABCG1 expression and cellular cholesterol efflux in THP-1 cells. RC may provide a novel tool for identifying subtype-function and drug development.
© 2005 Published by Elsevier B.V. on behalf of the Federation of European Biochemical Societies.

Keywords: Liver X receptor; ATP-binding cassette transporter A1; ATP-binding cassette transporter G1; HDL; Cholesterol

1. Introduction

The liver X receptors α and β (LXRα and LXRβ) are nuclear receptors that form obligate heterodimers with retinoid X receptor (RXR) [1]. LXRs are activated by several oxysterols or intermediates in the cholesterol synthetic pathway [2,3] and serve as key regulators of cholesterol homeostasis by coordinately regulating several genes involved in the efflux, transport, and excretion of cholesterol. These genes include ATP-binding cassette transporter (ABC) A1, ABCG1, and apolipoprotein E – which mediate cellular cholesterol efflux; cholesterol 7α-hydroxylase – the rate liming enzyme for the conversion of cholesterol to bile acids in the liver; and ABCG5/ABCG8–transporters involved in cholesterol /sterol excretion from the liver and intestine [1]. LXR activation also upregulates genes involved in fatty acid and triglyceride synthesis by inducing sterol regulatory element-binding protein-1c (SREBP-1c) – the master regulator of genes involved in lipogenesis [4–6] – and fatty acid synthase expression [7].

LXRα and LXRβ share a high degree of amino acid similarity (78%), have similar binding affinities to physiological oxysterol ligands [2,3], and have several common functions, including the upregulation of ABCA1 and ABCG1 expression [8,9]. However, these receptors have different tissue distributions: while LXRβ is ubiquitously expressed, the expression of LXRα is limited to the liver, kidney, intestine, adipose tissue, and macrophages [10]. In the liver, LXRα serves as an important regulator of cholesterol catabolism. Mice lacking LXRα has no resistance to dietary cholesterol and fail to upregulate hepatic cholesterol 7α-hydroxylase [11,12], whereas LXRβ null mice maintain their resistance. The role of LXR subtypes in triglyceride metabolism is uncertain. One study has shown a reduction in the liver triglyceride level of LXRβ null mice on standard diet [13], whereas a reduction in the expression of lipogenic genes was observed in LXRα null mice fed cholesterol [11,12]. Thus, selective agonists for each LXR subtype may be necessary to elucidate their precise functions.

Riccardin C (RC) and F (RF) are non-sterol natural products isolated from liverworts [14,15] (Fig. 1A). In the present study, we discovered that RC functions as an LXRα-selective agonist/LXRβ antagonist but effectively enhances cholesterol efflux from THP-1 cells.

2. Materials and methods

2.1. Riccardins C and F
RC and RF were purified from a methanol extract of the liverwort *Blasia pusilla* as described previously [14,15].

2.2. Transient transfections and reporter gene assay
CV-1 cells maintained in DMEM containing 10% FCS were co-transfected with 248 ng of LXR response element (LXRE)-driven luciferase vector (pLXRE$_X$4-tk-Luc), 248 ng of pSV-β-galactosidase control vector (Promega), and 1.25 ng each of pcDNA3.1-LXRα or LXRβ and pcDNA3.1-RXRα with Polyfect (Qiagen) in 24-well plates according to a previously described method [16]. Three hours after transfection, the cells were treated with test compounds in DMEM containing 10% delipidated FBS, 20 μM compactin, and 10 μM mevalonic acid for 24 h. The cells were then lysed and the reporter gene activity was determined. Luciferase activity was normalized to that of β-galactosidase for each well.

*Corresponding author.
E-mail address: mogami@nihs.go.jp (T. Nishimaki-Mogami).

Abbreviations: LXR, liver X receptor; RXR, retinoid X receptor; ABC, ATP-binding cassette transporter; SREBP-1c, sterol regulatory element-binding protein-1c; LXRE, LXR response element; 22(*R*)HC, 22(*R*)-hydroxycholesterol; TO-1317, TO-901317
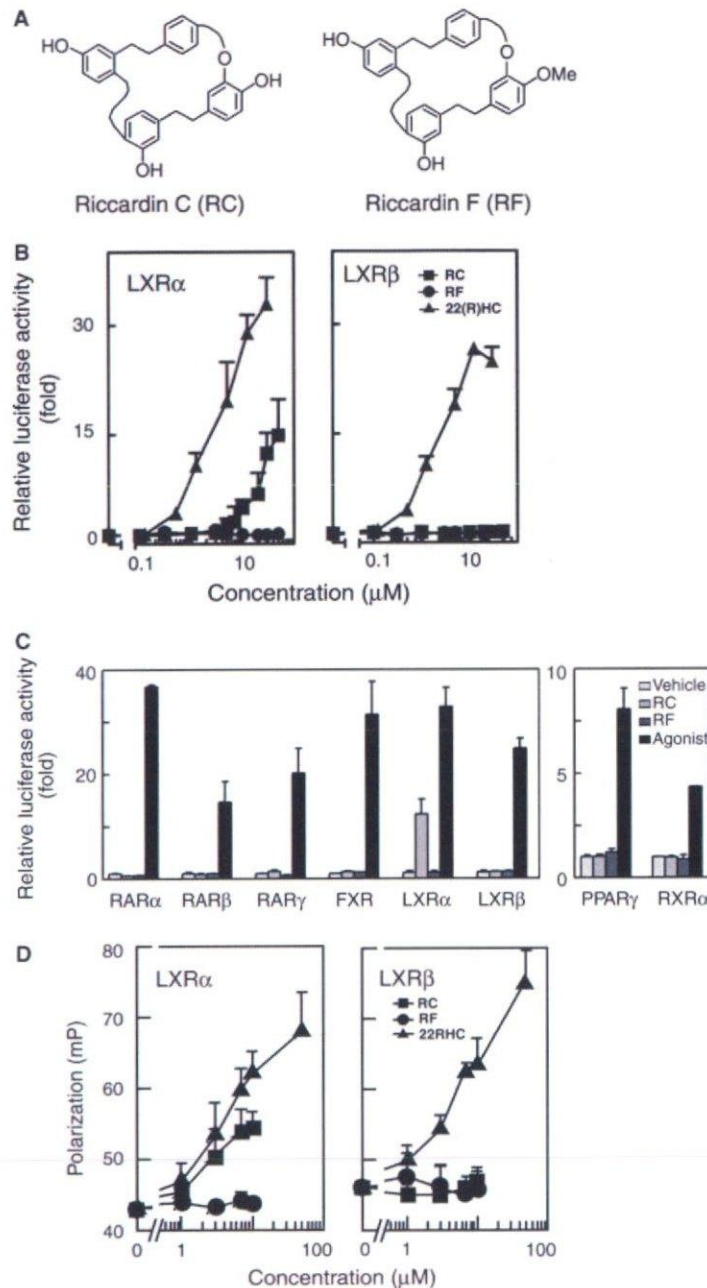
Fig. 1. RC activates LXRα but not LXRβ. (A) Chemical structures of RC and RF. (B) CV-1 cells were transfected with a reporter plasmid (pLXRE$_X$4-tk-*Luc*) and expression plasmids for LXRα (or LXRβ) and RXRα, together with a β-galactosidase as an internal control, and were treated for 24 h with various concentrations of RC, RF, or 22(R)HC. Luciferase activity in the cell extracts was normalized using β-galactosidase and expressed as the fold induction relative to vehicle-treated cells. The values are the means ± S.D. of six experiments. (C) Effects of RC and RF on transcriptional activities of heterodimers between RXRα and RARα, RARβ, RARγ, FXR, LXRα, or LXRβ, and RXRα homodimers. CV-1 cells were transfected with expression plasmids for receptors and a β-galactosidase together with a reporter plasmid (pDR5$_X$3-cmv-*Luc* for RARs, pFXRE$_X$4-tk-*Luc*, or pDR1$_X$4-cmv-*Luc* for RXRα), or a PPARγ-Gal4-expression plasmid with a pGal4-UAS-*Luc*. The cells were exposed to RC (30 μM), RF (30 μM), or receptor-specific agonists (3 μM all-trans retinoic acid for RARs and RXRα, 30 μM chenodeoxycholic acid for FXR, 20 μM 22(R)HC for LXRs, 30 μM ciglitazone for PPARγ) for 24 h before assaying luciferase activity. The values are the means ± S.D. (*n* = 3). (D) Purified GST-LXRα or GST-LXRβ ligand binding domain was incubated with a fluorescence-tagged SRC-1 peptide and various concentrations of RC, RF, or 22(R)HC. The association of ligand-induced SRC-1 peptide with the receptor was monitored by evaluating the increases in millipolarization fluorescence units (mP). The values are the means ± S.D. of six experiments.

2.3. Coactivator association assay using fluorescence polarization

A coactivator association assay using fluorescence polarization was performed according to a previously described method [16]. A TAMRA-labeled peptide (0.1 μM with the amino acid sequence ILRKLLQE) was incubated with purified 1.5 μM GST-fused human LXRα ligand binding domain or LXRβ ligand binding domain in 100 μl of buffer (10 mM HEPES, 150 mM NaCl, 2 mM MgCl$_2$, and 5 mM DTT at pH 7.9) in 96-well black polypropylene plates. After 1-h incubation at room temperature, ligand-dependent recruitment of the coactivator-peptide was measured as the increase in fluorescence polarization using a Fluorescence Plate Reader Fusionα (Perkin–Elmer Life Science).

2.4. Real-time quantitative reverse transcription-PCR

Gene-specific mRNA quantitation was performed by real-time RT-PCR on an ABI Prism 7700 sequence detection system (Applied Biosystems). THP-1 cells maintained in RPMI 1640 medium (Sigma) containing 10% FCS were subcultured in 6-well plates and treated with test compounds in RPMI 1640 containing 0.2% bovine serum albumin. Total RNA extracted from cells using an RNeasy Kit (Qiagen) was treated with DNase according to the manufacturer's instructions. The relative mRNA expression levels were determined using the TaqMan one-step RT-PCR Master Mix (PE Applied Biosystems). The primer/probe sequences for human ABCA1, ABCG1, and SREBP-1c have been previously reported [17].

2.5. Measurement of lipid efflux to apolipoprotein A-I

The lipid efflux measurements were performed according to a previously described method [18]. Briefly, THP-1 cells were treated with the test compounds and 0 or 10 μg/ml of human apoA-I, isolated from the plasma HDL fraction, in RPMI 1640 containing 0.2% bovine serum albumin for 24 h. The lipids were extracted and the cholesterol level was determined using enzymatic methods.

2.6. Statistical analysis

Data were analyzed by ANOVA followed by the Student–Newman–Keuls method.

3. Results

3.1. Identification of RC as an LXRα Agonist

To discover novel LXR agonists, we screened a variety of natural products using a transient transfection assay. CV-1 cells were cotransfected with an LXRE-driven luciferase reporter plasmid and expression plasmids for human LXRα (or LXRβ) and RXRα. RC and RF (Fig. 1A) are novel macrocyclic bis(bibenzyl) dimers isolated from the liverwort [14,15]. Upon cotransfection with LXRα/RXR, RC (30 μM) raised the transactivation of the reporter gene by approximately 15-fold, while a natural LXR agonist, 22(R)-hydroxycholesterol (22(R)HC), resulted in a 30-fold increase (Fig. 1B). At higher concentrations, RC caused a decrease in β-galactosidase activity. LXRβ/RXRα-dependent transactivation was unaffected by this compound. RF, a 14-methoxyl derivative of RC, activated neither LXRα nor LXRβ. Furthermore, neither RC nor RF activated heterodimers between RXRα and RARα, RARβ, RARγ, FXR, or PPARγ, and RXRα homodimers in cell-based luciferase assays (Fig. 1C).

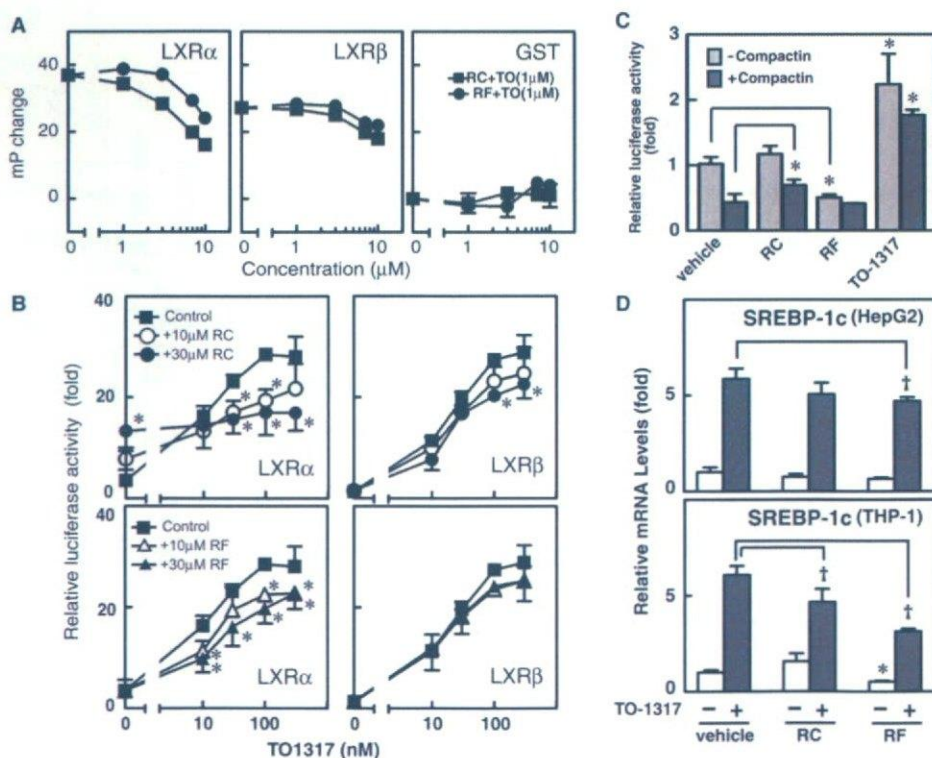In an in vitro coactivator-recruitment assay, RC (up to 10 μM) induced a dose-dependent interaction between SRC-1

Fig. 2. RC competes with endogenous or synthetic ligands for LXR activation. (A) Fluorescence-tagged SRC-1 peptide was incubated with GST-LXRα, GST-LXRβ, or GST. The changes in fluorescence polarization caused by 1 μM TO-1317 in the presence of the indicated concentrations of RC or RF are shown. A blank value in the absence of ligands was subtracted from the measured values. The values are the means ± S.D. (n = 3). (B) CV-1 cells were transfected with pLXREₓ4-tk-*Luc* and either LXRα/RXRα or LXRβ/RXRα plasmids, as shown in Fig. 1B, and treated for 24 h with various concentrations of TO-1317 with or without RC or RF (10 or 30 μM). The values are the means ± S.D. of three experiments performed in triplicate. Data were normalized to no ligand control (take as 1) and 100 nM TO-1317 values of a representative experiment. Significantly different from respective controls (*, P < 0.05). (C) HepG2 cells were transfected with pLXRE-tk-*Luc* and treated for 24 h with RC (30 μM) or TO-1317 (10 nM) with or without compactin (50 μM) and mevalonic acid (40 μM). The values are the means ± S.D. of three experiments performed in triplicate. Significantly different from respective controls (*, P < 0.05). (D) THP-1 cells and HepG2 cells were treated for 24 h with the vehicle (DMSO) alone, RC or RF (30 μM) in the presence or absence of 100 nM TO-1317. SREBP-1c mRNA level was measured by TaqMan quantitative real-time PCR. Data were normalized to 18S rRNA levels and are expressed as the fold induction relative to that in the vehicle-treated cells. The values are the means ± S.D. (n = 3). Significantly different from vehicle controls (*, P < 0.05) or cells treated with TO-1317 alone (†, P < 0.05).

peptide and LXRα but not LXRβ (Fig. 1D). At higher concentrations, RC caused non-specific interference in monitoring fluorescence polarization. No interactions were induced by RF.

3.2. RC and RF compete with synthetic or endogenous ligands for LXR activation

When assayed in the presence of 1 μM TO-1317 (TO-901317), RC and RF reduced the TO-1317-induced association of the SRC-1 peptide with LXRα or LXRβ, indicating the binding of these compounds to the receptors (Fig. 2A). These compounds also decreased LXRα-transactivation elicited by a synthetic LXR agonist TO-1317 (Fig. 2B), although inhibitory effect of RF on LXRβ was insignificant. The ability of RC and RF to compete with endogenous ligands was tested in HepG2 cells. Treatment of the cells with compactin, which has been reported to deplete endogenous ligands for LXR [19,20], led to a 60% reduction in LXRE-dependent transactivation (Fig. 2C). Similarly, RF decreased the luciferase activity to the level of cells treated with compactin. RC had no effect in the absence of compactin but increased luciferase activity by 1.6-fold in compactin-treated cells. RC and RF inhibited the TO-1317-elicited expression of SREBP-1c mRNA in THP-1 cells. RF also decreased the TO-1317-elicited expression in HepG2 cells, although the effect of RC was insignificant (Fig. 2D).

3.3. RC enhances ApoA-I-mediated cellular cholesterol release

We used real-time quantitative PCR to investigate the effect of RC on the expression of LXR target genes, ABCA1, ABCG1, and SREBP-1c, in THP-1 cells. RC (30 μM) increased the ABCA1 mRNA level by 2-fold, while 22RHC (12.5 μM) and TO-1317 (10 nM) caused 2.2- and 2.7-fold inductions, respectively (Fig. 3A). Likewise, RC raised the ABCG1 and SREBP-1c mRNA level by 2.6-fold and 1.6-fold, respectively.

To evaluate whether the increase in ABCA1 mRNA expression was functionally relevant, we examined the effect of RC on cholesterol efflux from THP-1 cells. As shown in Fig. 3B, apoA-I-dependent cholesterol release was increased 2-fold by 10 μM of RC. At 30 μM, this compound also caused a 2-fold elevation in cholesterol release without exogenous apoA-I.

RC had no effect on SREBP-1c and ABCG1 mRNA expression in HepG2 cells, whereas TO-1317 markedly induced expression of both of them (Fig. 3C).

4. Discussion

In the present study, we identified RC as an LXRα-selective agonist. RC bound directly to LXRα and recruited the coacti-
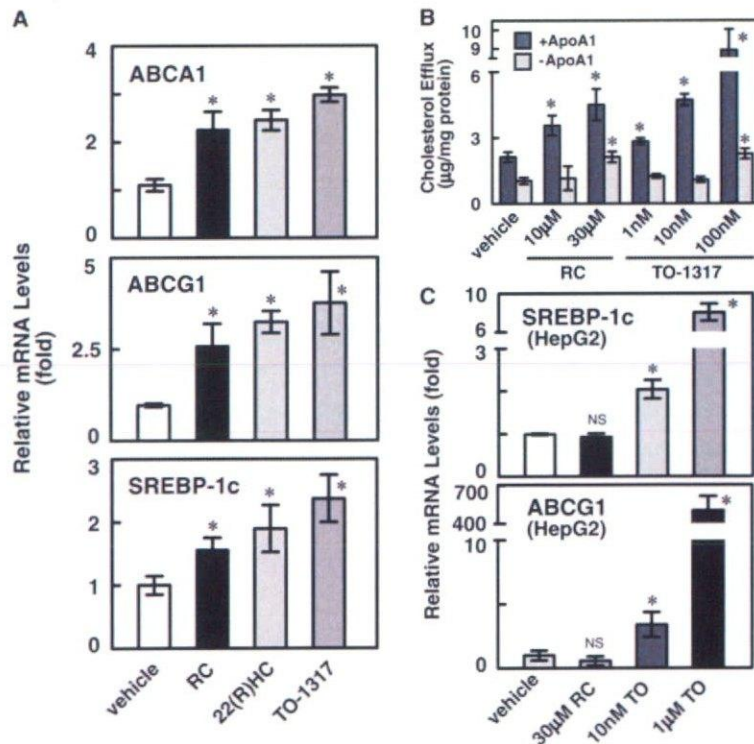

Fig. 3. RC increases ABCA1 and ABCG1 mRNA expression and cellular cholesterol efflux in THP-1 cells without raising SREBP-1c expression in HepG2 cells. (A) THP-1 cells were treated for 24 h with the vehicle (DMSO) alone, RC (30 μM), TO-1317 (10 nM), or 22(R)HC (12.5 μM). The levels of ABCA1 and ABCG1 mRNA were measured with TaqMan quantitative real-time PCR analysis. Data were normalized using the 18S rRNA levels and are expressed as the fold induction relative to that in the vehicle-treated cells. The values are the means ± S.D. of three experiments performed in triplicate. (B) Cells were treated for 24 h with the indicated compounds in the presence or absence of apoA-I (10 μg/ml), and the cholesterol released into the medium was analyzed. The values are the means ± S.D. (n = 3) of a typical series of three experiments performed. (C) HepG2 cells were treated for 24 h with the vehicle (DMSO) alone, RC (30 μM), or TO-1317 (10 nM or 1 μM). SREBP-1c and ABCG1 mRNA level was measured by quantitative real-time PCR. Data were normalized to 18S rRNA levels and are expressed as the fold induction relative to that in the vehicle-treated cells. The values are the means ± S.D. of three experiments. Statistically significant differences from control are indicated by asterisk (*, P < 0.05 and NS, not significant).

vator SRC-1 peptide to the receptor (Fig. 1D), leading to the activation of LXRα-dependent reporter gene transcription (Fig. 1B). RC also possesses the ability to bind to LXRβ. However, its inability to recruit a coactivator to LXRβ (Fig. 1D) resulted in the failure of LXRβ-mediated transactivation. RC was shown to have no ability to activate PPARγ, RARα, RARβ, RARγ, FXR, and RXRα (Fig. 1C).

In contrast to RC, RF was inactive for both LXRα and LXRβ-mediated transactivation (Fig. 1B). This compound was able to bind to LXRα and LXRβ (Fig. 2A) but was unable to promote coactivator association (Fig. 1C). Structural differences between RC and RF suggest that the C-14 hydroxyl group of RC plays a critical role in inducing coactivator association to LXRα, but not to LXRβ, leading to transactivation in a subtype-selective manner.

The competition with the synthetic agonist TO-1317 for the coactivator association (Fig. 2A) and the receptor-mediated transactivation (Fig. 2B) demonstrates that RC functions as an LXRα partial agonist and an LXRβ antagonist. RF functions as an antagonist of LXRα. RF decreased LXRE-dependent luciferase transcription in HepG2 cells to the level of endogenous-ligand depletion by compactin (Fig. 2C), suggesting that endogenous ligand-mediated LXR activation was inhibited by RF. RC increased LXRE-dependent transcription in compactin-treated cells, but not in the absence of compactin. In the intact cells, RC, as well as RF, might compete with endogenous ligands for LXR activation, thereby decreasing endogenous ligand-mediated activation. This latent activity of RC might compensate for this reduction. RC and RF also competed with TO-1317 for SREBP-1c expression in THP-1 cells.

The efflux of cellular cholesterol to HDL constitutes the first stage in the reverse cholesterol transport pathway and plays a critical role in modulating the progression of atherosclerosis [21]. ABCA1 and ABCG1 have been shown to mediate this process [22,23], and LXRα and LXRβ play redundant roles in their expression [9,24]. RC functions as an LXRα partial agonist and LXRβ antagonist. However, RC was shown to raise ABCA1 and ABCG1 mRNA levels and enhance cellular cholesterol efflux in THP-1 cells (Fig. 3A and B). Because human LXRα expression is autoregulated by LXRα itself [25], the stimulation of LXRα may have a stronger effect than that of LXRβ. RC and TO-1317 at higher concentrations increased cholesterol efflux even in the absence of apoA-I. Because THP-1 cells express apoE [26] and ABCA1 at the basal level, increased expression of apoE by LXR activation [27], caveolin-1 [28], or ABCA7 [29] could lead to enhanced cholesterol release, even without apoA-I.

We found that RC did not affect SREBP-1c and ABCG1 expression in hepatoma HepG2 cells (Fig. 3C). This coincides with the apparent inability of RC to enhance LXRE-dependent transactivation in this cell line (Fig. 2C). A possible explanation for this inability is the low LXRα/LXRβ ratio in HepG2 cells. Alternatively, as a partial LXRα agonist/LXRβ antagonist, RC might compete with endogenous ligands produced via the cholesterol synthesis pathway. It is also possible that coactivator-corepressor(s) different from those employed in THP-1 cells might be active in this cell line. Further studies are required to elucidate the precise mechanisms of RC's selective actions. However, because synthetic LXR agonists have been shown to cause hypertriglyceridemia [5], LXR modulators that do not upregulate hepatic lipogenic genes may enable improved therapeutic strategies.

References

[1] Edwards, P.A., Kast, H.R. and Anisfeld, A.M. (2002) BAREing it all: the adoption of LXR and FXR and their roles in lipid homeostasis. J. Lipid Res. 43, 2–12.

[2] Janowski, B.A., Willy, P.J., Devi, T.R., Falck, J.R. and Mangelsdorf, D.J. (1996) An oxysterol signalling pathway mediated by the nuclear receptor LXR alpha. Nature 383, 728–731.

[3] Lehmann, J.M., Kliewer, S.A., Moore, L.B., Smith-Oliver, T.A., Oliver, B.B., Su, J.L., Sundseth, S.S., Winegar, D.A., Blanchard, D.E., Spencer, T.A. and Willson, T.M. (1997) Activation of the nuclear receptor LXR by oxysterols defines a new hormone response pathway. J. Biol. Chem. 272, 3137–3140.

[4] Repa, J.J., Liang, G., Ou, J., Bashmakov, Y., Lobaccaro, J.M., Shimomura, I., Shan, B., Brown, M.S., Goldstein, J.L. and Mangelsdorf, D.J. (2000) Regulation of mouse sterol regulatory element-binding protein-1c gene (SREBP-1c) by oxysterol receptors, LXRalpha and LXRbeta. Genes Dev. 14, 2819–2830.

[5] Schultz, J.R., Tu, H., Luk, A., Repa, J.J., Medina, J.C., Li, L., Schwendner, S., Wang, S., Thoolen, M., Mangelsdorf, D.J., Lustig, K.D. and Shan, B. (2000) Role of LXRs in control of lipogenesis. Genes Dev. 14, 2831–2838.

[6] Yoshikawa, T., Shimano, H., Amemiya-Kudo, M., Yahagi, N., Hasty, A.H., Matsuzaka, T., Okazaki, H., Tamura, Y., Iizuka, Y., Ohashi, K., Osuga, J., Harada, K., Gotoda, T., Kimura, S., Ishibashi, S. and Yamada, N. (2001) Identification of liver X receptor-retinoid X receptor as an activator of the sterol regulatory element-binding protein 1c gene promoter. Mol. Cell Biol. 21, 2991–3000.

[7] Joseph, S.B., Laffitte, B.A., Patel, P.H., Watson, M.A., Matsukuma, K.E., Walczak, R., Collins, J.L., Osborne, T.F. and Tontonoz, P. (2002) Direct and indirect mechanisms for regulation of fatty acid synthase gene expression by liver X receptors. J. Biol. Chem. 277, 11019–11025.

[8] Costet, P., Luo, Y., Wang, N. and Tall, A.R. (2000) Sterol-dependent transactivation of the ABC1 promoter by the liver X receptor/retinoid X receptor. J. Biol. Chem. 275, 28240–28245.

[9] Venkateswaran, A., Repa, J.J., Lobaccaro, J.M., Bronson, A., Mangelsdorf, D.J. and Edwards, P.A. (2000) Human white/murine ABC8 mRNA levels are highly induced in lipid-loaded macrophages. A transcriptional role for specific oxysterols. J. Biol. Chem. 275, 14700–14707.

[10] Lu, T.T., Repa, J.J. and Mangelsdorf, D.J. (2001) Orphan nuclear receptors as eLiXiRs and FiXeRs of sterol metabolism. J. Biol. Chem. 276, 37735–37738.

[11] Alberti, S., Schuster, G., Parini, P., Feltkamp, D., Diczfalusy, U., Rudling, M., Angelin, B., Bjorkhem, I., Pettersson, S. and Gustafsson, J.A. (2001) Hepatic cholesterol metabolism and resistance to dietary cholesterol in LXRbeta-deficient mice. J. Clin. Invest. 107, 565–573.

[12] Peet, D.J., Turley, S.D., Ma, W., Janowski, B.A., Lobaccaro, J.M., Hammer, R.E. and Mangelsdorf, D.J. (1998) Cholesterol and bile acid metabolism are impaired in mice lacking the nuclear oxysterol receptor LXR alpha. Cell 93, 693–704.

[13] Schuster, G.U., Parini, P., Wang, L., Alberti, S., Steffensen, K.R., Hansson, G.K., Angelin, B. and Gustafsson, J.A. (2002) Accumulation of foam cells in liver X receptor-deficient mice. Circulation 106, 1147–1153.

[14] Yoshida, T., Hashimoto, T., Takaoka, S., Kan, Y., Tori, M. and Asakawa, Y. (1996) Phenolic constituents of the liverwort: four novel cyclic Bisbibenzyl dimers from *Blasia pusilla* L. Tetrahedron 52, 14487–14500.

[15] Hashimoto, T., Yoshida, T., Kan, Y., Takaoka, S., Tori, M. and Asakawa, Y. (1994) Structures of four novel macrocyclic Bis(bibenzyl) dimmers, pusilatins A–D from the liverwort *Blasia pusilla*. Tetrahedron Lett. 35, 909–910.

[16] Nishimaki-Mogami, T., Une, M., Fujino, T., Sato, Y., Tamehiro, N., Kawahara, Y., Shudo, K. and Inoue, K. (2004) Identification of intermediates in the bile acid synthetic pathway as ligands for the farnesoid X receptor. J. Lipid Res. 45, 1538–1545.